Emerging Laser Technologies for High-Power and Ultrafast Science

Online at: https://doi.org/10.1088/978-0-7503-2536-3

IOP Series in Coherent Sources, Quantum Fundamentals, and Applications

About the Editor

F J Duarte is a laser physicist based in Western New York, USA. His career has expanded three continents while contributing in the academic, industrial and defense sectors. Duarte is editor/author of 15 laser optics books and sole author of three books: *Tunable Laser Optics, Quantum Optics for Engineers*, and *Fundamentals of Quantum Entanglement*. Duarte has made original contributions in the fields of coherent imaging, directed energy, high-power tunable lasers, laser metrology, liquid and solid-state organic gain media, narrow-linewidth tunable laser oscillators, organic semiconductor coherent emission, *N*-slit quantum interferometry, polarization rotation, quantum entanglement, and space-to-space secure interferometric communications. He is also the author of the generalized multiple-prism grating dispersion theory and pioneered the use of Dirac's quantum notation in *N*-slit interferometry and classical optics. His contributions have found applications in numerous fields, including astronomical instrumentation, dispersive optics, femtosecond laser microscopy, geodesics, gravitational lensing, heat transfer, laser isotope separation, laser medicine, laser pulse compression, laser spectroscopy, mathematical transforms, nonlinear optics, polarization optics, and tunable diode laser design. Duarte was elected Fellow of the Australian Institute of Physics in 1987 and Fellow of the Optical Society of America in 1993. He has received various recognitions, including the *Paul F Foreman Engineering Excellence Award* and the *David Richardson Medal* from the Optical Society.

Coherent Sources, Quantum Fundamentals, and Applications

Since its discovery, the laser, has found innumerable applications from astronomy to… zoology. Subsequently, we have also become familiar with additional sources of coherent radiation such as the free electron laser, optical parametric oscillators, and coherent interferometric emitters. The aim of this book Series in Coherent Sources, Quantum Fundamentals, and Applications is to explore and explain the physics and technology of widely applied sources of coherent radiation and to match them with utilitarian and cutting-edge scientific applications. Coherent sources of interest are those that offer advantages in particular emission characteristics areas such as broad tunability, high spectral coherence, high energy, or high power. An additional area of inclusion are those coherent sources capable of high performance in the miniaturized realm. Understanding of quantum fundamentals can lead to new and better coherent sources and unimagined scientific and technological applications. Application areas of interest include the industrial, commercial, and medical sectors. Also, particular attention is given to scientific applications with a bright future such as coherent spectroscopy, astronomy, biophotonics, space communications, space interferometry, quantum entanglement, and quantum interference.

Publishing benefits
Authors are encouraged to take advantage of the features made possible by electronic publication to enhance the reader experience through the use of colour, animation and video, and incorporating supplementary files in their work.

Do you have an idea of a book that you'd like to explore?
For further information and details of submitting book proposals, see iopscience.org/books or contact Ashley Gasque at ashley.gasque@iop.org.

Emerging Laser Technologies for High-Power and Ultrafast Science

Edited by
François Légaré
Institut national de la recherche scientifique Centre Énergie Matériaux Télécommunications, Varennes, Québec, Canada

IOP Publishing, Bristol, UK

ISBN 978-0-7503-2536-3 (ebook)
ISBN 978-0-7503-2534-9 (print)
ISBN 978-0-7503-2537-0 (myPrint)
ISBN 978-0-7503-2535-6 (mobi)

DOI 10.1088/978-0-7503-2536-3

Version: 20210701

IOP ebooks

British Library Cataloguing-in-Publication Data: A catalogue record for this book is available from the British Library.

Published by IOP Publishing, wholly owned by The Institute of Physics, London

IOP Publishing, Temple Circus, Temple Way, Bristol, BS1 6HG, UK

US Office: IOP Publishing, Inc., 190 North Independence Mall West, Suite 601, Philadelphia, PA 19106, USA

Contents

Preface

High power, ultrafast laser technologies are now used for a wide variety of applications both in fundamental and applied research, touching many scientific disciplines including physics, chemistry, materials science, and biology, but also for societal applications including health, environmental, security, and defense. Ultrafast lasers have enabled major technological advances and are now widely used in industry.

Since 1985, the year when the chirped pulse amplification (CPA) technique was introduced by Strickland and Mourou [1], the peak power of ultrafast lasers has continuously grown reaching recently 10 PW [2], and intensities approaching 10^{23} W cm^{-2} are now available [3]. For more details, here is a recent review [4]. This technology is mostly based on the Titanium:Sapphire (Ti:Sa) amplification gain medium providing pulses of few tens of femtoseconds (fs) at 800 nm center wavelength. For millijoule (mJ) class laser systems, the pulse duration can be further reduced down the single-cycle regime (2.66 fs at 800 nm) using the hollow core fiber approach that was introduced 25 years ago by Nisoli and co-workers [5]. For sub-PW systems, recent progress with thin plate compression provides a route to reach sub-10 fs pulse duration and boost the peak power through a very efficient approach [6].

Over the last two decades, Ti:Sa technology has been the workhorse for ultrafast scientists enabling major breakthroughs that cannot all be discussed in a preface. One amazing outcome of this technology has been the generation of secondary sources from the THz to the hard x-ray spectral range, as well as high energy particles (electrons, ions, and neutrons) using compact laser-driven accelerator schemes. Among many outcomes, in 2021 we are celebrating the twentieth anniversary of the generation of isolated attosecond pulses, which has given rise to the field of attosecond science [7, 8]. Since these light pulses and particles are fully synchronized, sophisticated pump-probe experiments enable the tracking of complex ultrafast dynamics in matter such as attosecond electronic motion in atoms, molecules, and solids [9, 10].

In this context, scientists using ultrafast laser systems want to have access to more average power for generating secondary sources with higher brightness, including high repetition rates, over various regions of the electromagnetic spectrum to drive nonlinear processes that are wavelength dependent such as THz generation and high harmonic generation, to tunable sources to perform spectroscopy, as well as to shorter pulses to improve the temporal resolution of pump-probe experiments. With high repetition rate high average power lasers, one can compensate the low conversion efficiency of nonlinear processes used to generate secondary sources at extreme wavelengths. This book has been written to provide examples of recent achievements in ultrafast optics dealing with these requirements at the forefront of laser technologies.

Chapter 1 discusses the most recent achievements in terms of high energy, high average power laser systems, reporting the use of Ytterbium:YAG gain medium to generate picosecond pulses with kW of average power at kHz repetition rate for

Joule energy per pulse. These performances combine the highest pulse energy and average power to date, and will enable scaling by orders of magnitude the brightness of secondary sources driven by high energy pulses.

Motivated by nonlinear processes that are wavelength dependent, there are major efforts to develop ultrafast laser systems operating at longer wavelengths. In this context, chapters 2–4 discuss different strategies to achieve this goal. Chapter 2 presents the most recent development for high energy, high repetition rate fiber laser systems delivering ultrashort pulses at 2 μm center wavelength. Using thulium-doped fused-silica as a gain material, and benefitting from large core fibers, average power and peak power available nowadays have already reached the same as that obtained with the well-established Ytterbium fiber laser technology. This remarkable achievement paves a roadmap to provide 2 μm laser systems with 100 GW peak power (10 mJ with 100 fs pulse duration) at kW of average power (100 kHz).

Chapter 3 presents recent breakthroughs regarding the development of CPA based on chromium doped zinc selenide gain material (Cr^{2+}:ZnSe) delivering multi-mJ ultrashort pulses at 2.5 μm at kHz repetition rate. To seed the amplifier, the authors present a unique scheme to generate carrier-envelope phase (CEP) stable broadband pulses, resulting in the shortest pulse duration obtained from a Cr^{2+}:ZnSe laser amplifier (44 fs). With filamentation in air for spectral broadening, the bandwidth to generate 17.5 fs pulses is demonstrated. Such a laser system will be ideal to generate isolated attosecond pulses over the entire water window spectral range, even reaching the L-edges of ferromagnetic materials.

In chapter 4, a recent laser technology enabling high repetition rate (100 kHz) tunable narrowband and broadband laser pulses in the infrared and mid-infrared spectral range is presented. Using optical parametric chirped pulse amplification (OPCPA) pumped by high average power Yb:YAG lasers, tens of Watts of average power are available at long wavelengths. This technology, commercialized by Fastlite, capitalizes on their proprietary device called the Dazzler, an acousto-optic programmable dispersive filter that enables to manage the dispersion in the OPCPA to maximize efficiency and reach Fourier transform limited pulse duration over the tunable range. Furthermore, this unique device enables one to switch instantaneously between two modes of operation, i.e., tunable narrow spectral bandwidth for spectroscopic applications and ultrashort CEP stable mid-IR pulses.

Chapter 5 describes the efforts being made to reach the few-optical-cycle regime for ultraviolet pulses. The main route to achieve this task is to exploit low dispersion gas media for frequency up-conversion of Ti:Sa and Ytterbium:YAG laser sources. UV generation methods to obtain few-fs (sub 3-fs) pulse duration are discussed, providing state-of-the-art UV sources as a key ingredient in the field of ultrafast UV spectroscopy. Applications to study in real time the ultrafast response of photo-excited states of matter are discussed by the authors.

To the readers, I really hope that you will enjoy reading this book as much as I did. Even though I have been working in this research field for 20 years, I am always amazed by the progress that is made and by laser scientists, through their ingenuity and hard work, who push the limits and specification of ultrafast laser technologies. As a community, we can envision performances that will enable breakthroughs in

fundamental and applied research, thus enabling innovations and new laser based technologies for societal applications.

References

[1] Strickland D and Mourou G 1985 Compression of amplified chirped optical pulses *Opt. Commun.* **55** 447–9

[2] Doria D *et al* 2020 Overview of ELI-NP status and laser commissioning experiments with 1 PW and 10 PW class-lasers *J. Instrum.* **15** C0903

[3] Yoon J W *et al* 2019 Achieving the laser intensity of 5.5×1022 W cm^{-2} with a wavefront-corrected multi-PW laser *Opt. Express* **17** 20413

[4] Danson C N *et al* 2019 Petawatt and exawatt lasers worldwide *High Power Laser Sci. Eng.* **7** e54

[5] Nisoli M *et al* 1996 Generation of high energy 10 fs pulses by a new pulse compression technique *Appl. Phys. Lett.* **68** 2793

[6] Mironov S Y *et al* 2020 Thin plate compression of a sub-petawatt Ti:Sa laser pulses *Appl. Phys. Lett.* **116** 241101

[7] Drescher M *et al* 2001 X-ray pulses approaching the attosecond frontier *Science* **291** 1923–7

[8] Hentschel M *et al* 2001 Attosecond metrology *Nature* **414** 509–13

[9] Krausz F and Ivanov M 2009 Attosecond physics *Rev. Mod. Phys.* **81** 163–234

[10] Young L *et al* 2018 Roadmap of ultrafast X-ray atomic and molecular physics *J. Phys. B: At. Mol. Opt. Phys* **51** 032003

Editor biography

François Légaré

Institut national de la recherche scientifique, Centre Énergie Matériaux Télécommunications, Varennes, Québec, Canada

François Légaré, PhD in chemistry from the Université de Sherbrooke (2004), has joined the Institut national de la recherche scientifique—Énergie Matériaux Télécommunications centre in 2006. Since 2013, he has been the director of the Advanced Laser Light Source user facility.

The general goal of his research is to use nonlinear optical phenomena to develop novel ultrafast light sources and approaches to image and control matter.

Légaré is a Fellow and senior member of the Optical Society (2017) and a member of The College of New Scholars, Artists and Scientists of the Royal Society of Canada (2017). He was awarded the Herzberg medal from the Canadian Association of Physics (2015) and the Rutherford Memorial Medal in physics of the Royal Society of Canada (2016). He has contributed to more than 160 articles in peer reviewed journals and has been invited to more than 70 conferences and workshops. He has also contributed to intellectual properties with 4 patents, 4 in national phases, and 1 US provisional. Furthermore, he is fostering the transfer of technologies to Canadian spin-off companies, including *few-cycle* Inc. (founded in 2013, 8 employees) and FemtoGate (founded in 2019). Since 2006, he has enthusiastically supervised and supported 37 internships, 9 MSc and 16 PhD students, and 22 postdoctoral fellows. Currently, his team is composed of 2 MSc, 8 PhD, 7 postdoctoral fellows, 2 research associates, 3 technicians, and 3 research engineers.

List of contributors

Olivier Albert
Fastlite, Pôle Euro 95—Bât D, 165 rue des Cistes, 06600 Antibes, France

Cory Baumgarten
XUV Lasers Inc., Fort Collins, CO 80525, USA

Francesca Calegari
Center for Free-Electron Laser Science CFEL, Deutsches Elektronen-Synchrotron DESY, Notkestraße 85, 22607 Hamburg, Germany

Physics Department, Universität Hamburg, Luruper Chaussee 149, 22761 Hamburg, Germany
The Hamburg Centre for Ultrafast Imaging, Universität Hamburg, Luruper Chaussee 149, 22761 Hamburg, Germany

Andrea Cartella
The Hamburg Centre for Ultrafast Imaging, Universität Hamburg, Luruper Chaussee 149, 22761 Hamburg, Germany

Zenghu Chang
University of Central Florida, Orlando, FL, USA

Han Chi
XUV Lasers Inc., Fort Collins, CO 80525, USA

Lorenzo Colaizzi
Center for Free-Electron Laser Science CFEL, Deutsches Elektronen-Synchrotron DESY, Notkestraße 85, 22607 Hamburg, Germany

Physics Department, Universität Hamburg, Luruper Chaussee 149, 22761 Hamburg, Germany

Kristian Dehne
XUV Lasers Inc., Fort Collins, CO 80525, USA

Nicolas Forget
Fastlite, Pôle Euro 95—Bât D, 165 rue des Cistes, 06600 Antibes, France

Christian Gaida
Active Fiber Systems GmbH, Ernst-Ruska Ring 17, 07745 Jena, Germany

Martin Gebhardt
Institute of Applied Physics, Friedrich-Schiller University Jena, Albert Einstein Str. 15, Beutenberg Campus, 07745 Jena, Germany

Cesar Jauregui
Institute of Applied Physics, Friedrich-Schiller University Jena, Albert Einstein Str. 15, Beutenberg Campus, 07745 Jena, Germany

Esben Larsen
Imperial College London, London SW7 2BW, UK

Jialin Li
University of Central Florida, Orlando, FL, USA

Jens Limpert
Institute of Applied Physics, Friedrich-Schiller University Jena, Albert Einstein Str. 15, Beutenberg Campus, 07745 Jena, Germany

Fraunhofer Institute for Applied Optics and Precision Engineering, Albert Einstein Str. 7, 07745 Jena, Germany

Raman Maksimenka
Fastlite, Pôle Euro 95—Bât D, 165 rue des Cistes, 06600 Antibes, France

Alphonse Marra
University of Central Florida, Orlando, FL, USA

Carmen S Menoni
XUV Lasers Inc., Fort Collins, CO 80525, USA

Brendan A Reagan
XUV Lasers Inc., Fort Collins, CO 80525, USA

Jorge J Rocca
XUV Lasers Inc., Fort Collins, CO 80525, USA

Daniel Schade
Imperial College London, London SW7 2BW, UK

Nicolas Thiré
Fastlite, Pôle Euro 95—Bât D, 165 rue des Cistes, 06600 Antibes, France

Andrea Trabattoni
Center for Free-Electron Laser Science CFEL, Deutsches Elektronen-Synchrotron DESY, Notkestraße 85, 22607 Hamburg, Germany

Lifeng Wang
University of Central Florida, Orlando, FL, USA

Yong Wang
XUV Lasers Inc., Fort Collins, CO 80525, USA

Vincent Wanie
Center for Free-Electron Laser Science CFEL, Deutsches Elektronen-Synchrotron DESY, Notkestraße 85, 22607 Hamburg, Germany

Yi Wu
University of Central Florida, Orlando, FL, USA

Fangjie Zhou
University of Central Florida, Orlando, FL, USA

IOP Publishing

Emerging Laser Technologies for High-Power and Ultrafast Science

François Légaré

Chapter 1

High energy, high average power ytterbium lasers

Jorge J Rocca, Yong Wang, Han Chi, Cory Baumgarten, Brendan A Reagan, Kristian Dehne and Carmen S Menoni

1.1 Introduction

Since the invention of the laser, higher pulse energy, greater average power, and shorter pulse duration are constantly evolving frontiers that create new applications and even open entire new fields. The peak power of lasers has increased over the years at a rate that compares with the dramatic increase of the number of transistors in semiconductor chips (Moore's law), at present reaching 10 PW [1]. Impressive increases have also been achieved in pulse energy, with lasers now delivering nanosecond pulses of more than one megajoule [2]. Dramatic reductions in pulse durations have also been realized with laser pulses with hundreds of joules being produced in the femtosecond regime [1]. However, the average power of joule-level ultrashort pulse lasers has, until very recently, remained low. There are important applications in science and technology in which progress depends on the development of compact lasers capable of producing ultrashort laser pulses of high energy at high repetition rate. These applications include coherent and incoherent plasma-based sources of extreme ultraviolet, soft and hard x-rays photons, and the production of gamma rays by inverse Compton scattering. Also, high power, ultrashort pulse lasers operating at repetition rates at and above 1 kHz are required for the implementation of compact particle accelerators based on laser wakefield acceleration for fundamental research and applications. These and other applications motivate the development of high average power, short pulse lasers at institutions worldwide.

Figure 1.1 summarizes the current state-of-the-art of high energy, high average power, short pulse (<10 ps) lasers operating at wavelengths near 1 μm, which is, at present, the wavelength range that has produced the highest average powers.

doi:10.1088/978-0-7503-2536-3ch1

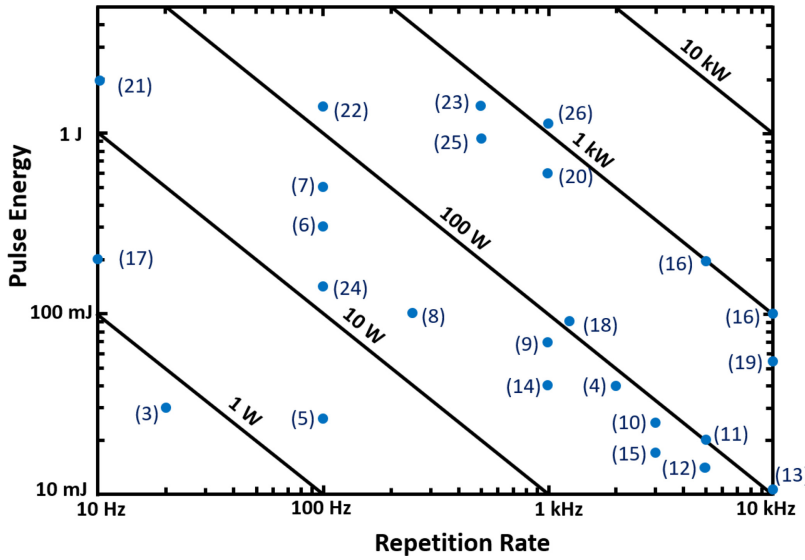

Figure 1.1. Summary of state-of-the-art diode-pumped Yb-doped lasers at $\lambda \approx 1$ μm with high pulse energy (>10 mJ) and repetition rate of up to 10 kHz with pulses compressible to sub-10 ps duration. Each number identifies work listed in the reference section [3–26].

Different approaches, all of them enabled by pumping with laser diodes, have been investigated. The gain geometry has been in the form of slabs, thin disks, or thicker disks operating at cryogenic temperatures. Another approach uses the coherent combination of the output of fiber lasers. Most of these lasers are based on diode-pumping of Yb:YAG, a mature gain material that is readily available and that combines high heat conductivity, large stimulated emission cross section, and relatively broad bandwidth. Yb:YAG picosecond lasers have already reached a pulse energy of 1 J at a repetition rate of 1 kHz, and further increases in both the average power and the pulse energy are expected.

In this chapter we discuss the material properties of Yb:YAG in comparison with other Yb host materials, followed by a summary of its characteristics at cryogenic temperature relative to room temperature. This is followed by a discussion of the state-of-the-art high average power, high energy, thin disk lasers and cryogenic Yb:YAG lasers.

1.2 Yb-doped gain media

The advent of highly efficient, high power semiconductor laser diodes with narrow band emission which better matches the absorption of solid state laser materials than flash lamps has enabled important advances in high power lasers. It has resulted in greatly increased efficiency, larger average power, increased compactness, and reliability. However, a limitation of laser diodes as compared to traditional flash lamps is their relatively low peak power. This requires using gain media with long upper level lifetime that can efficiently store the pump energy. Numerous laser

materials with adequate laser upper level lifetime for pumping with laser diodes have been investigated or are under development. The two rare earth ion dopants, neodymium and ytterbium, have so far dominated the development of high power lasers. They are well suited for diode pumping due to the inherent wavelength matching between their absorption bands and that of commercially available high power diodes. Nd^{+3} can be efficiently pumped by λ = 790–900 nm InGaAsP/GaAs or AlGaAs/GaAs laser diodes, and Yb^{+3} by λ = 900–980 nm InGaAs/GaAs laser diodes. Yet Yb^{3+} materials such as Yb:YAG have the advantage of having an upper level lifetime of ~1 ms, which is over four times longer than similar Nd^{3+} materials like Nd:YAG, which has a lifetime of 230 μs. This allows for better pump energy usage, and therefore reduced cost. Furthermore, when pumped at λ = 942 nm Yb:YAG has an absorption bandwidth of 18 nm full width at half maximum (FWHM) [27], which is nearly an order of magnitude greater than the 2 nm absorption bandwidth of Nd:YAG at λ = 808 nm. This relaxes diode linewidth and center wavelength stability requirements.

Figure 1.2 shows the energy level diagrams for Nd^{3+} and Yb^{3+}. In both materials lasing takes place at wavelengths around 1 μm in transitions between the $^4F_{5/2}$ and $^4I_{11/2}$ manifolds in Nd^{3+} and between the $^2F_{5/2}$ and $^2F_{7/2}$ manifolds in Yb^{3+}. A first observation is the different value of the quantum defect between the two materials, i.e., the difference between pump and emission wavelengths. When expressed as the fraction of the lasing wavelength to the pump wavelength, Nd:YAG has a quantum defect of 24% when pumped at 808 nm, while Yb:YAG has a value of 9% when pumped at 942 nm. This is significant because the quantum defect is often the primary direct source of heating in the material. Therefore, minimizing the lasing to pump wavelength difference is key for high power laser operation, where thermal

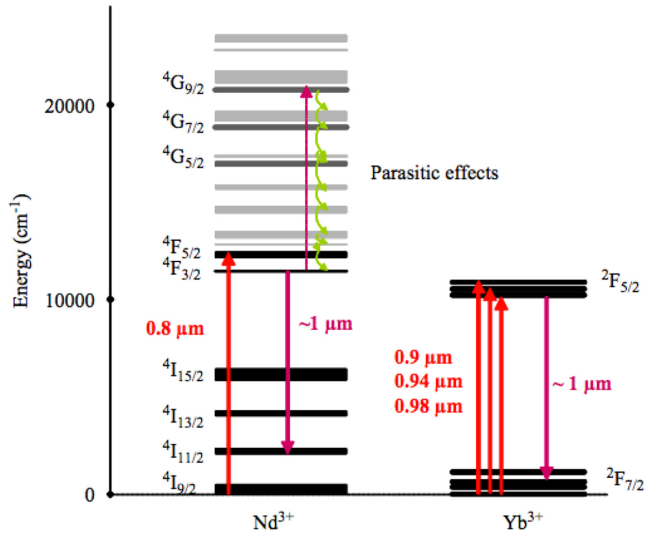

Figure 1.2. The relevant energy levels of Nd^{3+} and Yb^{3+} gain media with typical pump and lasing transitions, as well as parasitic effects. Reprinted from Chenais *et al* [27], Copyright 2006, with permission from Elsevier.

management is one of the major challenges. Yb^{3+} also has a simplified electronic energy level diagram that helps to avoid most parasitic effects such as energy transfer upconversion, excited state absorption, and cross-relaxation, which all occur in Nd-doped media because of the existence of higher energy levels [27]. The main de-excitation paths of these high energy levels are primarily non-radiative and contribute to further thermal loading of the system. These deleterious effects can also depopulate the laser upper level, therefore reducing the population inversion and the gain. Finally, an advantage for the development of ultrafast lasers is the broader laser line emission bandwidth of Yb-doped materials, that is about an order of magnitude broader than of Nd-doped materials, allowing for the generation of shorter transform limited laser pulses. This broader gain bandwidth combined with longer storage lifetime comes with the consequence of lower peak stimulated emission cross section and the corresponding higher saturation fluence. Additionally, the small quantum defect results in a non-negligible thermal population on the lower laser level which increases threshold pumping requirements. However, as we discuss below, these complications are ameliorated at cryogenic operating temperatures. Overall, the Yb^{3+} ion has emerged over Nd^{+3} as a prime candidate for high repetition rate, high power, ultrafast laser development.

Numerous Yb-doped gain media with different host materials exist that exhibit many of the spectroscopic properties discussed above. These materials have long upper level lifetimes, τ_L, and small quantum defects, but differences in material properties make some more suitable than others for high power operation. These materials include Yb:YAG, Yb:KYW, Yb:KGW, Yb:YLF, and Yb:CaF_2. Some of their spectroscopic and mechanical properties are listed in table 1.1.

Several of these materials have been explored as options for high power lasers [33–36]. Hosts such as YLF and CaF_2 are attractive due to their broad emission bandwidth, $\Delta\lambda$, and good thermal conductivities, κ, and could constitute alternatives for high energy femtosecond lasers. These materials have found use in short pulse high power oscillators [37] and low energy amplifiers [3, 13, 38]. Yb:CaF_2 has also been used in diode-pumped high energy amplifiers [39, 40] to generate laser pulses of up to 54 J at repetition rates of less than 1 Hz, compressible to ~100 fs. Yet, its low stimulated emission cross section, σ_e, means it has a low gain, and a high saturation fluence. The saturation fluence of Yb:CaF_2 can exceed 100 J cm^{-2}, which is well

Table 1.1. Spectroscopic and mechanical properties of various Yb-doped materials. From S Chenais *et al* [27]. Other values have also been reported [28–32].

Crystal host	λ_e (nm)	λ_{abs} (nm)	$\Delta\lambda$ (nm)	σ_e (10^{-20} cm^2)	τ_L (ms)	κ (W m^{-1} K^{-1}) (undoped)
YAG	1030	942	9	2.1	0.95	11
KYW	1025	981	24	3	0.3	3.3
KGW	1023	981	20	2.8	0.3	3.3
YLF	1030	959	14	0.81	2.21	4.3
CaF_2	1049	980	70	0.25	2.4	9.7

above the damage threshold of optical coatings and even of the host material itself. This is a significant limitation for its use in the implementation of high average power, high energy amplifiers, where it is necessary to operate above the saturation fluence for efficient energy extraction. In the case of KYW and KGW, their low thermal conductivities have limited their use to mode-locked oscillators [41, 42] and low energy amplifiers [33, 34]. Of the available host materials, Yb:YAG, which has relatively high thermal conductivity and comparatively low saturation fluence, has emerged as the most utilized material for high energy, high repetition rate picosecond laser operation. Yttrium aluminum garnet ($Y_3Al_5O_{12}$), or YAG, has been a popular host material for decades due to its attractive spectroscopic, mechanical, and thermal properties. YAG has a body-center cubic lattice that makes it optically isotropic. However, thermal stress can still cause depolarization. YAG also has a higher fracture strength than most laser materials and is well suited to accept substitution of trivalent rare earth ions. Furthermore, since YAG has been studied as a laser host since the mid-1960s [43] and has found wide use with Nd^{3+} and Yb^{3+} dopants, the fabrication of high quality single crystal and ceramic YAG is mature, making large aperture YAG-based gain media commercially available. In recent decades, Yb:YAG has found wide use in high power picosecond chirped pulse amplification (CPA) lasers using a number of different designs including water-cooled thin disks [14–16], slabs [19, 44], and thicker disks or slabs operating at cryogenic temperatures [23–26]. Cryogenic Yb:YAG is particularly well suited for high pulse energy operation at high repetition rates.

1.2.1 Yb:YAG at cryogenic temperatures

The thermo-optical and mechanical properties of Yb:YAG as a gain medium for high power lasers improve greatly at cryogenic temperature [28, 45–47]. From table 1.1, we see that at room temperature YAG has a thermal conductivity of 11 W m^{-1} K^{-1}, which is better than many of the other host materials listed. However, it is still significantly worse than other host materials like sapphire used in Ti:Sapphire lasers, which has a thermal conductivity of 33 W m^{-1} K^{-1} at room temperature. Nevertheless, when cooled to cryogenic temperatures, the thermal conductivity of undoped YAG increases by nearly a factor of 9 with respect to room temperature. While this advantage is reduced when moderate levels of doping are introduced, a significant improvement of 3–5 times still remains [28]. In addition, as shown in table 1.2, the thermal expansion coefficient as well as the thermo-optic coefficient improve at cryogenic temperatures. The former is reduced by a factor of 4 as the temperature decreases from 300 K to 77 K, while the thermo-optics coefficient decreases by a factor of 7. In addition, the emission spectrum of Yb:YAG is significantly narrower at 77 K, which leads to an increase of the stimulated emission cross section and the corresponding decrease in the saturation fluence to below 2 J cm^{-2} [46]. This decrease in saturation fluence allows for efficient energy extraction without optical damage to the coatings and bulk materials. The associated increase in gain also allows for efficient energy extraction in a low number of passes through the gain media, which helps to avoid high nonlinear phase accumulation. On the

Table 1.2. Optical and mechanical properties of Yb:YAG at room temperature and at liquid nitrogen temperature. The column to the right quantifies the change. Values according to references [28, 45–47].

Yb:YAG properties at room and cryogenic temperature	300 K	77 K	Factor
Thermal conductivity (W m^{-1} K^{-1})	10	90	× 9
Thermo-optic coefficient (10^{-6}/K)	7.8	0.9	× 1/7
Expansion coefficient (10^{-6}/K)	6.14	1.95	× 1/4
Saturation fluence (J cm^{-2})	9.2	1.7	× 1/7

other hand, the narrower spectral bandwidth limits the shortest pulsewidth that can in practice be obtained to a few picoseconds. Therefore, several high energy cryo-cooled Yb:YAG laser system designs that suffer bandwidth narrowing in the amplifier chains have used hybrid approaches that combine either different cryogenically-cooled Yb-doped amplifier materials [18] or cryogenically-cooled power amplifiers with a room temperature first amplification stage where most of the gain takes place [23, 48].

A disadvantage of Yb:YAG's simple two manifold electronic structure and low quantum defect is that the lower laser level is thermally populated at room temperature. From Maxwell–Boltzmann statistics, the fraction of ions in the lower laser level has a population of 5.3% at 300 K due to thermal excitation from the ground state. This makes room temperature Yb:YAG a quasi-three level laser (figure 1.3(left)). Since there is an overlap between the absorption and emission bands, this leads to significant re-absorption and to a reduction of the effective emission bandwidth [28]. Therefore, there is a minimum amount of pump energy required for the system to reach transparency, and a corresponding reduction in the laser efficiency. This changes greatly when Yb:YAG is cooled to cryogenic temperatures, i.e., at ~77 K, liquid nitrogen temperature. At this temperature the fraction of ions in the lower laser level is reduced to 10^{-5}, making Yb:YAG a four level laser system (figure 1.3(right)), in which a population inversion and gain start to build up at low pump energy.

1.3 Thin disk lasers

The thin disk laser concept for the implementation of high average power diode-pumped solid state lasers, which dates back to 1994 [49], is illustrated in figure 1.4. The approach consists in the use of an active medium in the shape of a thin disk, typically 100–300 μm thick, that is cooled through one of the flat faces which is bonded to a water-cooled heat sink. The cooled face is coated with a dielectric multilayer stack that is highly reflective for both the pump and the laser wavelengths, while the opposite side of the disk is coated with an anti-reflection coating at both wavelengths. This geometry, which acts as a mirror with gain, is known as an 'active mirror', which can be used in reflection in an oscillator or amplifier. As the pump spot size is typically much larger than the disk thickness, one-dimensional heat flow results in which the temperature gradients are mainly coaxial to the disk

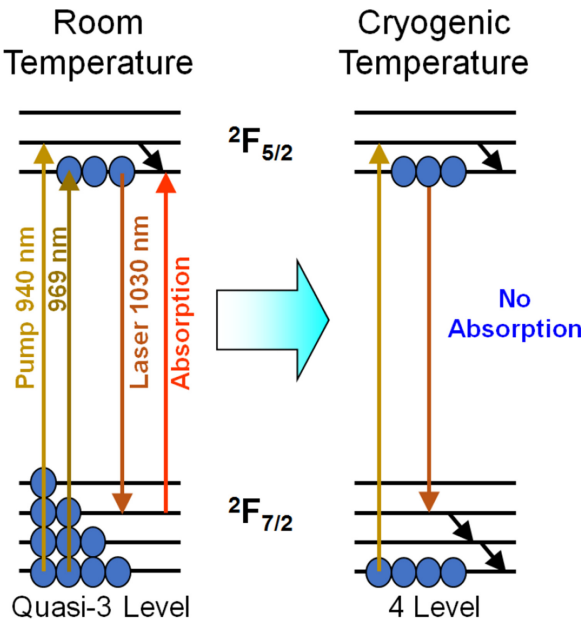

Figure 1.3. Population of the laser lower level in Yb:YAG at room and cryogenic temperature. The laser material changes from a quasi-three level system at room temperature (left) into a four level system at cryogenic temperature (right).

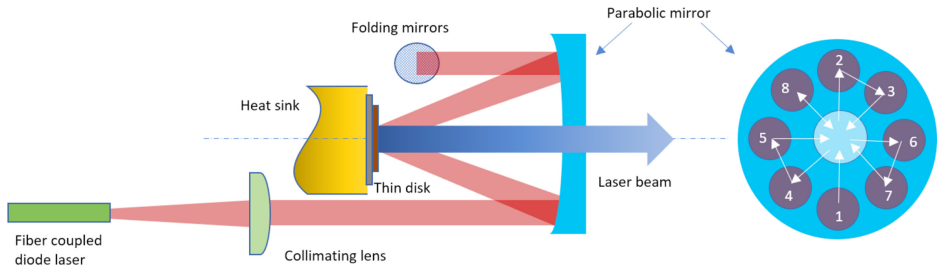

Figure 1.4. (a) Schematic illustration of the thin disk configuration for 16 pump passes. © 2007 IEEE. Reprinted, with permission, from Giesen *et al* [50].

and the laser beam. Therefore, the thermal lens effect can be greatly reduced with respect to an edge-cooled rod geometry, allowing for power scaling. Also, the large surface-to-volume ratio allows for efficient heat dissipation from the active medium into the heat sink, enabling operation at very high power densities.

Because of the small crystal thickness only a small fraction of the pump power is absorbed, requiring multiple passes of the seed beam through the gain medium. Figure 1.4 shows a typical arrangement to increase the number of pump beam passes through the crystal employing a parabolic mirror and a set of prism retro-reflectors. After each pass, the unabsorbed portion of the pump beam is collimated again by the other side of the parabolic mirror that focuses it onto the disk. This re-imaging is repeated until all the positions of the parabolic mirror are covered, the point at

which the pump beam can be redirected back to the source, thereby doubling the number of passes through the thin disk. This provides a platform for efficient pumping in which more than 90% of the pump power is absorbed in the disk. The small thickness also results in a small single pass gain that for efficient amplification requires multiples passes either in a resonator of a multi-pass amplifier configuration (figure 1.5(a)), or in a regenerative amplifier (figure 1.5(b)).

1.3.1 High energy thin disk regenerative amplifiers

The thin disk configuration has been used with Yb:YAG to create high average power regenerative amplifiers with output pulse energy of up to 100–200 mJ at repetition rates of 5–10 kHz [16]. This 1 kW average power CPA regenerative amplifier system used the architecture illustrated in figure 1.6(a) [16]. Pulses of 1.3 μJ energy from a Kerr-mode-locked thin disk oscillator are stretched to 1.5 ns duration in a grating stretcher. The stretched pulses are amplified to 1–2 mJ in a first thin disk regenerative amplifier. A following main amplifier is built around two diode-pumped water-cooled Yb:YAG thin disk amplifier heads that constitute the gain media in the ring-type resonator illustrated in figure 1.6(b). CW pump diodes

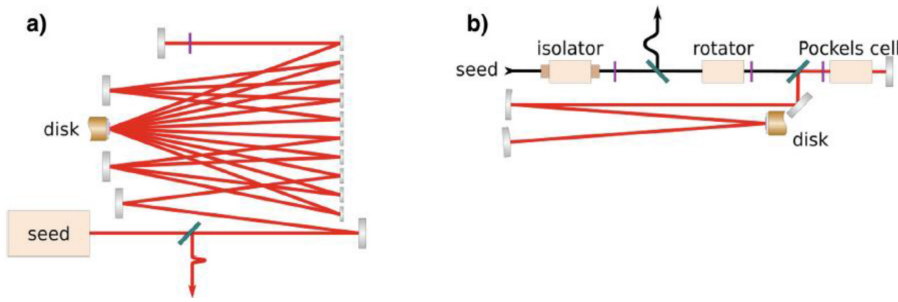

Figure 1.5. Schematic representation of (a) multi-pass amplifier, and (b) thin disk regenerative amplifier. From Saraceno *et al* [51] (2019). With permission of Springer.

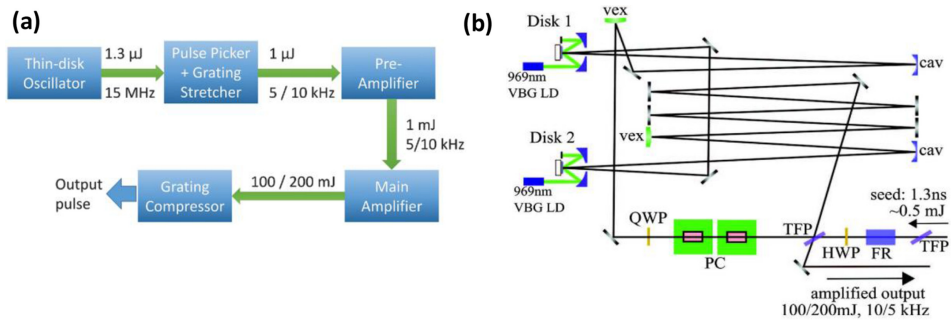

Figure 1.6. (a) Architecture of a kW average power 100–200 mJ thin disk regenerative amplifier. (b) Optical setup of the regenerative amplifier. QCW, quarter-wave plate; HWP, half-wave plate; FR, Faraday rotator; PC, Pockels cell; TFP, thin-film polarizer. VEX denotes a 10 m radius of curvature convex mirror; and CAV is a 15 m radius of curvature concave mirror. Reprinted with permission from Nubbemeyer *et al* [16] © The Optical Society.

operating at wavelengths of 969 nm are used to pump 6.8 mm spots into the 200 μm thick thin disks. The pump diodes are stabilized by volume Bragg gratings to enable direct pumping of the upper laser level via the narrow bandwidth zero phonon line. The resonator mode is symmetric with respect to the position of the two laser disks, ensuring similar mode size in both crystals. The first regenerative amplifier is used to increase the seed pulse energy to avoid chaotic behavior and achieve stable operation of the main amplifier.

As shown in figures 1.7(a) and (b), this system produces average powers exceeding 1 kW with the 100–200 mJ output pulse energies mentioned above. The spectral bandwidth of the pulses seeding the pre-amplifier is 3.5 nm and is reduced to 1.5 nm by gain narrowing in the two subsequent amplifier stages (figure 1.7(b)). The pulses were compressed to 1.08 ps using an efficient dielectric grating compressor. Another thin disk regenerative amplifier implementation has produced uncompressed pulses of slightly higher energy, 300 mJ, at 100 Hz repetition rate, that were subsequently compressed to 1.8 ps FWHM pulses of >240 mJ energy [52].

1.3.2 Thin disk multi-pass amplifiers

Thin Yb:YAG disks have also been used to implement high average power, multi-pass amplifiers which provide a platform to further increase the pulse energy. Outputs with compressed pulses of up to 720 mJ at 1 kHz repetition rate have been reported [20]. The laser system that produced these pulses is schematically illustrated in figure 1.8. It combines a commercially available regenerative amplifier that is based on a ring configuration, figure 1.8(b), with a multi-pass amplifier, both pumped by $\lambda = 940$ nm laser diodes as shown in figure 1.8(c).

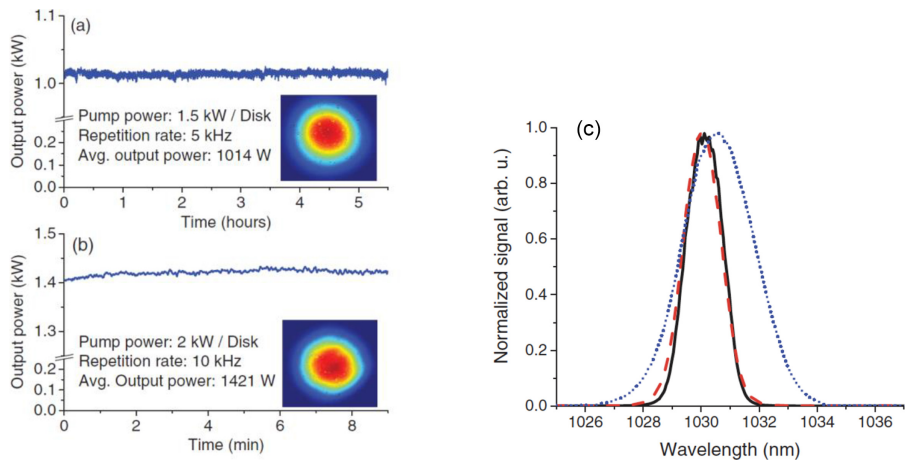

Figure 1.7. (a) Output power of thin disk regenerative amplifiers at 5 kHz repletion rate. (b) Output power at 10 kHz repetition rate achieved over several minutes. The insets show the measured output beam profiles for each repetition rate. (c) Spectra at the output of each of the stages of the regenerative amplifier depicted in figure 1.6: stretched seed pulse (blue dotted line), 1 mJ pre-amplifier output (red dashed line), and output of the main amplifier (black solid line). Reprinted with permission from Nubbemeyer *et al* [16] © The Optical Society.

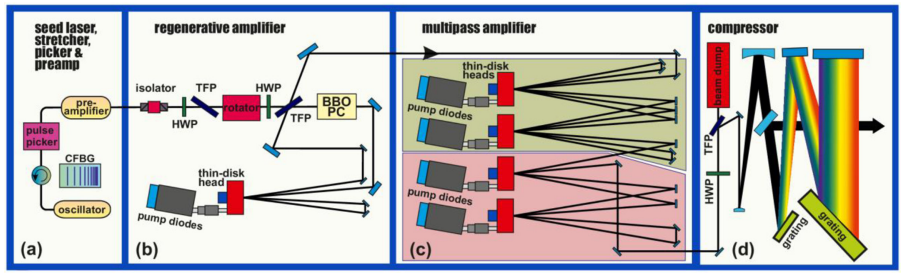

Figure 1.8. Thin disk laser system producing 720 mJ compressed pulses at 1 kHz repetition rate based on a thin disk regenerative amplifier followed by a multi-pass amplifier that uses four thin disks' amplifier heads. TFP, thin-film polarizer; HWP, half-wave plate; BBO PC, BBO-based Pockels cell. Reprinted with permission from Herkommer *et al* [20] © The Optical Society.

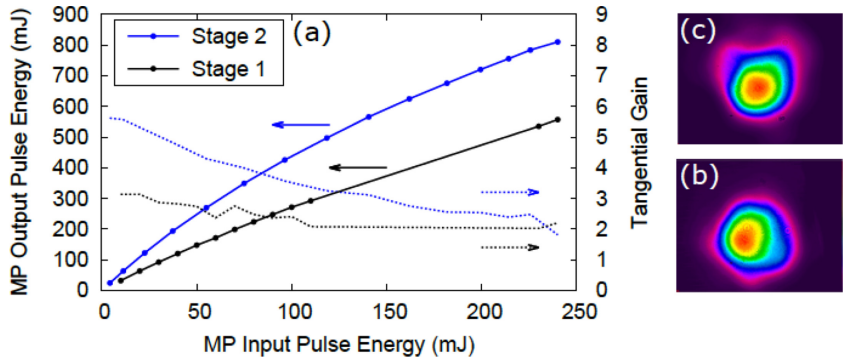

Figure 1.9. (a) Output pulse energy amplification characteristics of the two stages of the thin disk multi-pass amplifier of figure 1.8 as a function of seed pulse energy. The pump power is kept constant. (b) and (c) show the beam profiles after stage 1 and 2, respectively. Reprinted with permission from Herkommer *et al* [20] © The Optical Society.

The multi-pass amplifier is arranged in two stages, each made of two amplifier heads. A total average accumulated pump power of >9 kW is absorbed in the four water-cooled amplifier heads. The thermal lens at the operation point is compensated to obtain near-collimated propagation. The approach allows guiding of the seed beam over the thin disks multiple times with adjustable beam diameters using mirrors which are selected depending on the evolving beam size and divergence. Figure 1.9 shows the measured pulse output energy of each amplification stage as a function of seed pulse energy, maintaining constant pump power. In the first stage of this multi-pass amplifier, 240 mJ pulses from the regenerative pre-amplifier are amplified in two laser heads to 550 mJ in seven passes. In the second stage, the pulse energy is further increased to 800 mJ by four additional disk reflections. The pulses exiting the multi-pass amplifier are compressed into 720 mJ pulses of 0.92 ps duration in a dielectric grating compressor. The M^2 at the output of the amplifier was measured to be 1.89/2.32 in the major/minor axis.

1.4 Cryogenically-cooled Yb:YAG amplifiers

A different approach for the development of high energy, high average power amplifiers takes advantage of the improved thermo-optical and laser properties of Yb:YAG at cryogenic temperatures. The design architecture and performance of a compact $\lambda = 1.03$ μm CPA laser developed at Colorado State University based on cryogenically-cooled active mirror Yb:YAG amplifiers that produces pulses of up to 1.5 J at a repetition rate of 500 Hz is described below. The output pulses are compressed in vacuum to <5 ps in a dielectric grating compressor, yielding pulse energies of up to 1 J. A more recent implementation has produced 1.1 J picosecond pulses at 1 kHz repetition rate [26].

The approach relies on cryogenically-cooled Yb:YAG active mirrors. Although in these amplifiers the thickness of the gain medium (a few millimeters) is significantly larger than in the thin disk lasers, they share some of the same advantages. The geometry is still sufficiently thin to develop mostly longitudinal thermal gradients, reducing thermal lensing as compared to radially-cooled gain geometries. It also limits the maximum temperature difference within the gain region while its moderate diameter-to-length ratio reduces amplified spontaneous emission (ASE) depletion of the amplifier storage energy [53]. The improved thermal parameters at cryogenic temperatures compensate for the larger thickness of this geometry. Compared with thin disk lasers, the increased absorption reduces the number of passes necessary to efficiently absorb the pump, simplifying the design.

A block diagram showing the layout of the 500 Hz repetition rate, 1 J, picosecond laser system is shown in figure 1.10(a). The laser front-end is composed of a semiconductor saturable absorber mirror (SESAM) mode-locked Yb:KYW oscillator, a grating pulse stretcher, and a room temperature Yb:YAG regenerative amplifier. Since

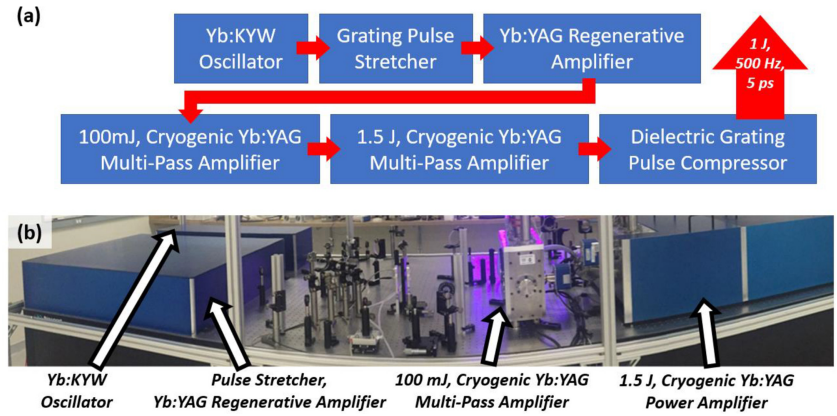

Figure 1.10. (a) Diagram of the laser system based on a high power, cryogenically-cooled Yb:YAG amplifier. The output of a diode-pumped, mode-locked bulk Yb:KYW oscillator is stretched by a grating stretcher and amplified to the millijoule level by a room temperature Yb:YAG regenerative amplifier. These seed pulses are subsequently amplified by a chain of two high power cryogenic amplifiers, and are compressed in vacuum by a dielectric grating pair. (b) Panoramic photograph of the high energy, high average power laser. Reproduced with permission from Reagan *et al* [54] © Cambridge University Press.

Yb:KYW is well suited to pumping by $\lambda = 980$ nm laser diodes, the crystal is pumped by a 30 W laser diode operating at that wavelength coupled to a 200 μm core fiber. The femtosecond pulses produced at 55 MHz repetition rate by the Yb:KYW oscillator are stretched by a 1740 line/mm grating to ~270 ps duration. The first stage of amplification is a room temperature Yb:YAG regenerative amplifier. This amplifier has the highest gain of any in the system, approximately 10^6, and is therefore where pulses suffer the most gain narrowing. Therefore, the choice of room temperature operation allows for a broader bandwidth [46]. Because of the mismatch between the center wavelength and the bandwidth of room temperature and cryogenic Yb:YAG, the stretcher is adjusted to select a spectral bandwidth that matches the region of peak gain in the subsequent cryogenic amplifiers while striking for a compromise between maximum pulse energy and broad spectral bandwidth at the exit of the final amplifier. Pulses leaving the grating stretcher seed the regenerative amplifier cavity via a thin-film polarizer (TFP). The active medium is a 0.5 mm thick, 10%-at. doped Yb:YAG active mirror soldered to a water-cooled copper heat sink. The Yb:YAG disk is pumped by ~200 W pulses of 200 μs duration from a fiber-coupled $\lambda = 940$ nm semiconductor laser diode. The stretched pulses suffer gain narrowing during amplification, and their pulse duration becomes 270 ps. These pulses can be compressed to ~2 ps durations, but their bandwidth is reduced when the wavelength is tuned to match the peak gain of the subsequent cryogenic amplifiers. The millijoule-level pulses are first amplified to about 100 mJ in a cryo-cooled pre-amplifier, and finally to the Joule level in the main multi-pass amplifier.

1.4.1 100 mJ pre-amplifier

The layout of the 100 mJ-level amplifier is shown in figure 1.11(a). A 5 mm thick, 2%-at. Yb:YAG active mirror is mounted on a cryogenic cooling manifold enclosed in a vacuum chamber. The highly reflective face of the active mirror is cooled by flowing cryogenic liquid at 77 K [23]. The Yb:YAG active mirror is pumped by $\lambda = 940$ nm, 500 μs duration pulses produced by two 400 W peak power fiber-coupled laser diode modules. A pump spot diameter of ~3.5 mm was used, and the pump radiation is absorbed in a single pass (one reflection).

The seed pulses from the laser front-end make four passes through the amplifier. Figure 1.11(b) shows the measured pulse energy exiting the amplifier as a function of pump energy at 500 Hz repetition rate. As can be seen from this plot, an amplified pulse energy of 100 mJ (50 W average power) is obtained when pumped with 360 mJ at 500 Hz repetition rate. These pulses have a bandwidth of 0.43 nm FWHM (figure 1.11(c)) and were compressed to 3.8 ps FWHM duration as shown by the SHG autocorrelation of figure 1.11(d).

1.4.2 High repetition rate, 1.5 J amplifier

The Joule-level amplifier is shown in figure 1.12(a). Two Yb:YAG active mirrors are mounted on a single cryogenic cooling head. The active mirrors are composites consisting of a 30 mm × 30 mm × 2 mm thick 3%-at. Yb:YAG crystal optically bonded on the four lateral faces to an absorbing Cr^{4+}:YAG cladding to reduce feedback of transversely emitted ASE and avoid parasitic oscillations. The front face

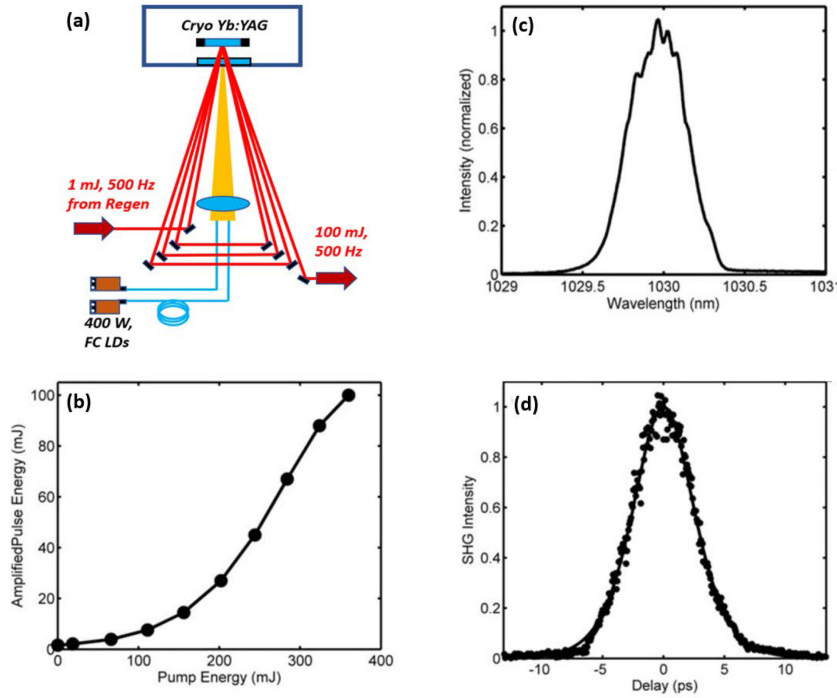

Figure 1.11. (a) Schematic layout of a 100 mJ, 500 Hz cryogenic amplifier. (b) Measured pulse energy at 500 Hz repetition rate as a function of total pump pulse energy. (c) Spectrum of the amplified pulses showing a bandwidth of 0.43 nm FWHM. (d) Autocorrelation of the compressed 100 mJ pulses at 500 Hz repetition rate. The sech^2 fit shown corresponds to a pulse duration of 3.9 ps FWHM. Reproduced with permission from Reagan *et al* [54] © Cambridge University Press.

of the assembly is bonded to an undoped YAG cap to further reduce ASE and to add mechanical stability. As shown in figure 1.12(a), each active mirror is pumped by pulses of 500 μs duration from a $\lambda = 940$ nm 6 kW laser diode stack. The pump beam diameter is ≈16 mm, and is double-passed to achieve >95% absorption. Seed pulses are injected into the amplifier through a TFP and are directed to pass through each active mirror twice. After double-passing a quarter-wave plate, the seed pulses pass back through the amplifier along the same path, achieving a total of four passes through each active mirror before being ejected from the amplifier by reflecting off the TFP. The amplifier occupies a table area of just over 0.5 m^2.

Figure 1.13 shows the performance characteristics of this amplifier operating at 500 Hz repetition rate. The laser output pulse energy as a function of total pump energy is displayed in figure 1.13(a). An output energy of 1.5 J (750 W average power) is obtained with an optical-to-optical efficiency of 37%. Figure 1.13(b) shows the measured output pulse energy stability over 30 min of continuous operation at 500 Hz repetition rate. A mean pulse energy of 1.4 J was obtained with an RMS deviation of 0.75%. Figure 1.13(c) shows a measured M^2 parameter of ~1.3 on both axes. The good beam quality in the far field is illustrated in figure 1.13(d). The pulses were compressed with about 70% efficiency by a pair of 1740 mm^{-1} dielectric

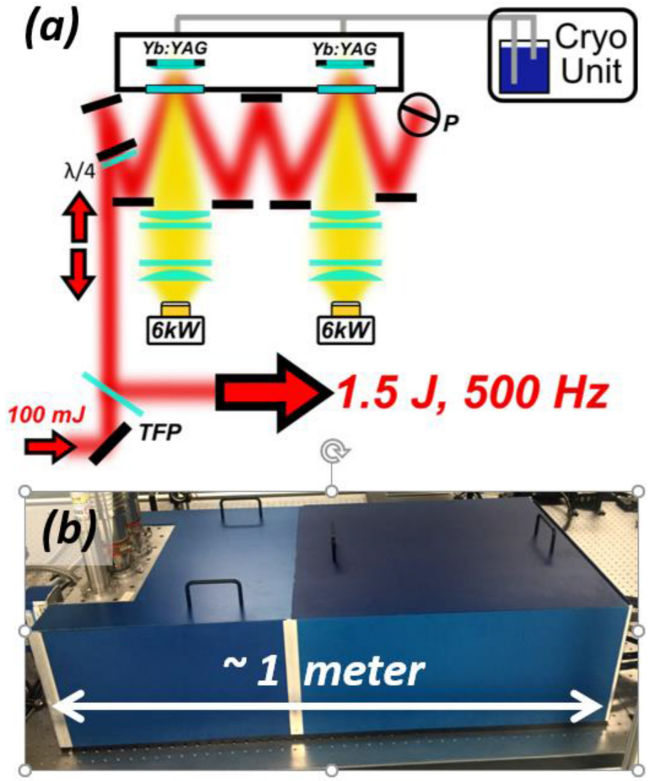

Figure 1.12. (a) Layout of the high repetition rate, 1.5 J amplifier. (b) Photo of the enclosed amplifier, which occupies a table space of just over 1 m × 0.5 m. TFP, thin-film polarizer; $\lambda/4$, quarter-wave plate; P, periscope; 6 kW laser diode stacks. Reproduced with permission from Reagan *et al* [54] © Cambridge University Press.

diffraction gratings. The resulting pulses had an energy of 1 J and a duration of ~5 ps at 500 Hz repetition rate, generating an average power of 0.5 kW.

1.4.3 1.1 J, 1 kHz repetition laser picosecond Yb:YAG laser

A different version of this system resulted in the first demonstration of a picosecond laser emitting >1 J pulses at 1 kHz repetition rate [26]. This cryogenically-cooled system generates pulses with >1.2 J energy at a repetition rate of 1 kHz, corresponding to an average power of 1.26 kW. After compression with high efficiency dielectric gratings, 1.1 J pulses with a duration of 4.5 ps were generated with good beam quality and high shot-to-shot stability. A schematic of this kW average power CPA picosecond laser system is illustrated in figure 1.14. It consists of a room temperature front-end that generates 2 mJ seed pulses followed by two cryogenic amplification stages and a vacuum dielectric grating compressor.

Differing from the 500 Hz system [23], the room temperature, thin disk regenerative Yb:YAG amplifier is pumped at its zero phonon line by 500 μs pulses from a 969 nm wavelength 60 W fiber-coupled laser diode. An 8-pass pump geometry forms a well-overlapped pump area of 1 mm diameter with a pump

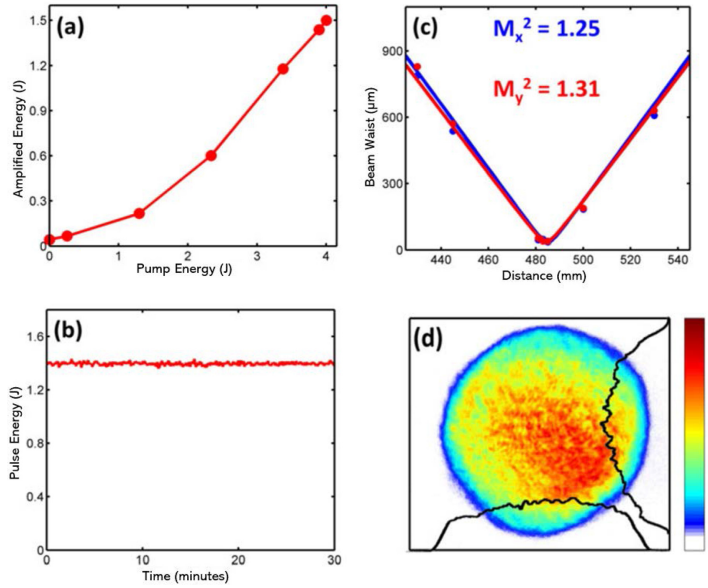

Figure 1.13. (a) Measured pulse energy exiting the main amplifier at 500 Hz repetition rate as a function of combined pump energy. (b) Amplified pulse energy over 30 min of continuous operation at 500 Hz repetition rate. A mean energy of 1.4 J was measured with an RMS fluctuation of 0.75%. (c) M^2 measurement in two orthogonal directions of the amplified output producing 1.4 J at 500 Hz repetition rate. (d) Far-field beam image of the full power output. Reproduced with permission from Reagan *et al* [54] © Cambridge University Press.

absorption of over 95%. A plano-concave cavity allows for four passes through the gain medium per round trip. The pre-amplifier consists of two active mirrors based on 5 mm thick 2%-at. Yb:YAG crystals mounted into a single evacuated chamber where their back surfaces are cooled by flowing liquid nitrogen. The number of active mirrors in this pre-amp was increased to two to better distribute the thermal load and to allow for a longer effective gain medium. A total of seven passes achieves the desired amplification to 100 mJ pulse energy at 1 kHz repetition rate. The first of the two active mirrors is pumped by imaging the output of a 400 W, $\lambda = 940$ nm, fiber-coupled diode laser into a 4 mm diameter spot. The laser pulses are amplified in five passes through the first crystal and are subsequently further amplified in two passes through the second active mirror that is pumped into a similar spot by two 400 W fiber-coupled laser diodes. For both crystals, the pump pulse duration is set at 450 μs. The ~100 mJ pulses are passed through an 8 mm diameter serrated aperture (SA) to achieve a nearly flat-top beam profile and pass through a Faraday rotator before injection into the final dual crystal cryogenic amplifier. Each crystal in this final amplifier stage is pumped at $\lambda = 940$ nm by a 6 kW diode array. The pump diodes generate 380 μs duration pulses at 1 kHz that are shaped to form nearly flat-top 16-mm-diameter pump profiles onto each active mirror. The temperature at the center of the pump region was measured to remain below 130 K (figure 1.15) using a spectroscopic technique [55]. After the seed pulses pass twice through each of the two active mirrors, a periscope is used to spatially rotate the beam 90 degrees and change its height. The beam is sent back to the two active

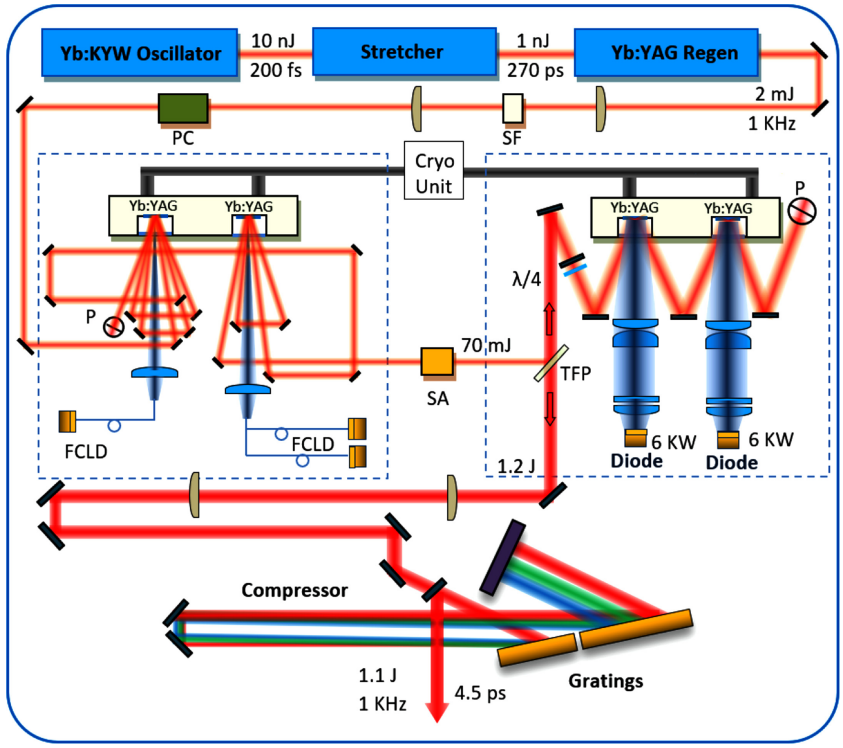

Figure 1.14. Schematic of the diode-pumped high energy CPA laser system. Regen, regenerative amplifier; SF, spatial filter; PC, Pockels cells; FCLD, fiber-coupled laser diodes; SA, serrated aperture; TFP, thin-film polarizer; P, periscope. Reprinted with permission from Wang *et al* [26] © The Optical Society.

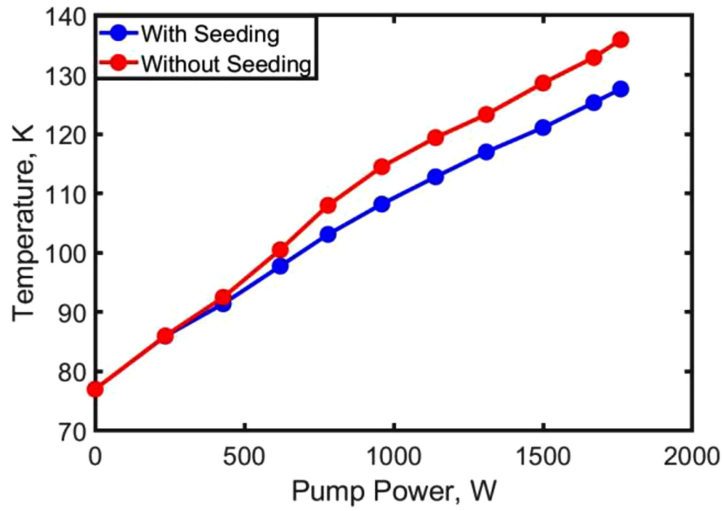

Figure 1.15. Measured temperature of one Yb:YAG active mirror in the final amplifier at the center of the pump with and without seeding vs. pump power. Reprinted with permission from Wang *et al* [26] © The Optical Society.

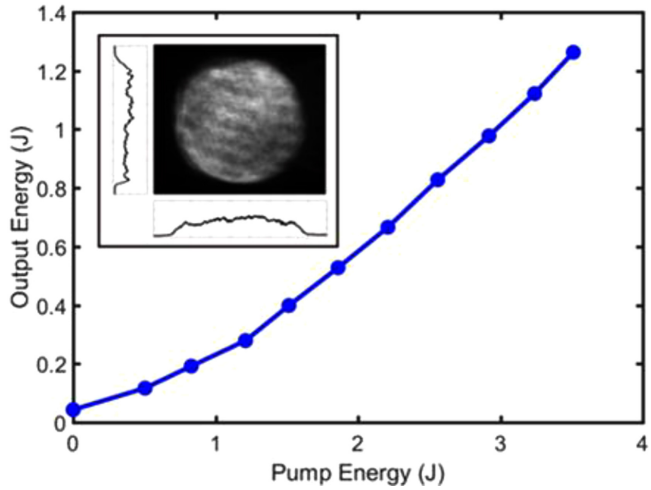

Figure 1.16. Measured laser pulse energy exiting the final amplifier as a function of total pump energy at 1 kHz repetition rate. A maximum energy of 1.26 J was obtained with a total pump energy of 3.5 J incident on the Yb:YAG active mirror. The inset shows the beam profile at 1 kHz, 1.26 kW average power. Reprinted with permission from Wang *et al* [26] © The Optical Society.

mirrors for the third and fourth pass. After the first four passes a quarter-wave plate combined with a 0-degree high reflector (HR) mirror rotates the polarization 90 degrees, sending the beam back through the same path to the TFP to exit the amplifier.

Figure 1.16 shows the measured output pulse energy as a function of the final amplifier total pump energy at 1 kHz repetition rate. A maximum 1.26 J pulse energy (1.26 kW average power) was obtained with a total pump pulse energy of 3.5 J. The optical-to-optical conversion efficiency is ~36%. The pulse-to-pulse energy stability is characterized by a standard deviation of 0.6%. As also shown by the inset in figure 1.16, the 1.26 kW average power output beam has a uniform flat-top profile. The beam is characterized by a measured $M^2 = 1.32$ and 1.39 on the horizontal and vertical directions, respectively (figure 1.17).

Figure 1.18(a) shows the measured spectra before the pre-amplifier and after the main amplifier. A 0.35 nm FWHM bandwidth is obtained at the output of the final amplifier stage, showing a minimal amount of gain narrowing, which supports a transform limited pulse duration of 3.9 ps (sech^2). Following amplification the beam is magnified to a diameter of ~40 mm and pulses are compressed with ~90% efficiency as shown by the SHG autocorrelator sech^2 fit in figure 1.18(b) corresponding to a pulse duration of 4.48 ps FWHM. The demonstrated 1.2 kW average power amplifier chain also provides the opportunity to generate nanosecond lasers pulses by substituting the short pulse laser front-end with one generating seed pulses of nanosecond duration.

1.4.4 Frequency-doubled 1 J Yb:YAG laser with 1 kW average power

The output of $\lambda = 1.030$ μm Yb:YAG lasers can be efficiently frequency-doubled to drive high pulse energy femtosecond sources based on Ti:Sapphire or optical

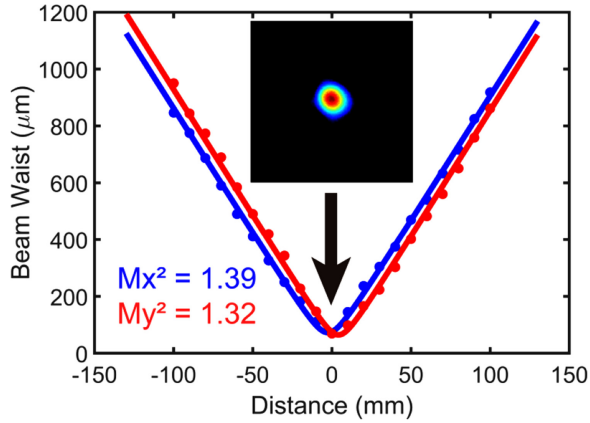

Figure 1.17. M^2 measurement of the 1.2 J, 1 kHz repetition rate output beam. The inset image shows the far-field beam profile at focus. Reprinted with permission from Wang *et al* [26] © The Optical Society.

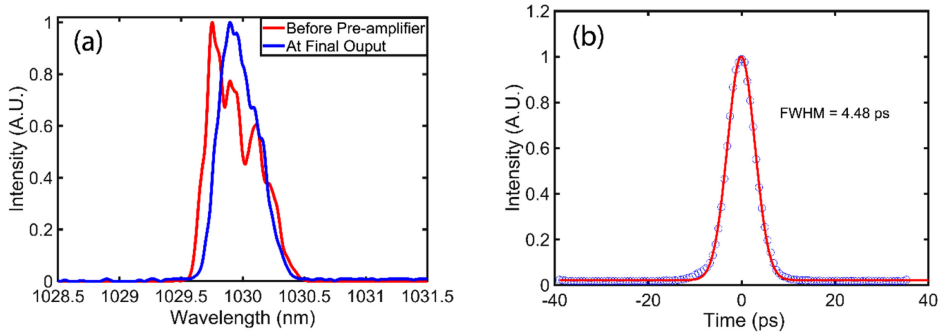

Figure 1.18. (a) Measured spectra at the input of the pre-amplifier (red) and the output of the final amplifier (blue). The pulses have an amplified bandwidth of 0.35 nm FWHM. (b) Second-harmonic autocorrelation after pulse compression. The solid trace is the sech^2 fit with a width corresponding to a pulse duration of 4.48 ps. Reprinted with permission from Wang *et al* [26] © The Optical Society.

parametric chirped pulse amplifiers (OPCPA) at kHz repetition rates. Most of the progress achieved in the development of high average power green lasers based on Yb:YAG has been limited to the generation of μJ to mJ-level pulses at repetition rates ranging from hundreds of kHz to MHz [56, 57]. For example, 370 W average power at $\lambda = 515$ nm was achieved by the generation of 7 μJ pulses at 50 MHz repetition rate [56]. An average power of 1.4 kW at the same wavelength was achieved with 4.8 mJ pulses at 300 kHz repetition rate [57]. In comparison, the repetition rate and average power of lasers generating Joule-level green pulses has remained considerably lower until recently. SHG in the DIPOLE laser based on a cryogenically-cooled Yb:YAG laser has produced 5.6 J pulses at 10 Hz repetition rate, an average power of 56 W [58]. SHG in yttrium calcium oxyborate (YCOB) of pulses from the Yb:S-FAP Mercury laser produced 31.7 J at 10 Hz repetition rate (317 W average power) [59]. A 1 kHz cryogenically-cooled Yb:YAG laser similar to

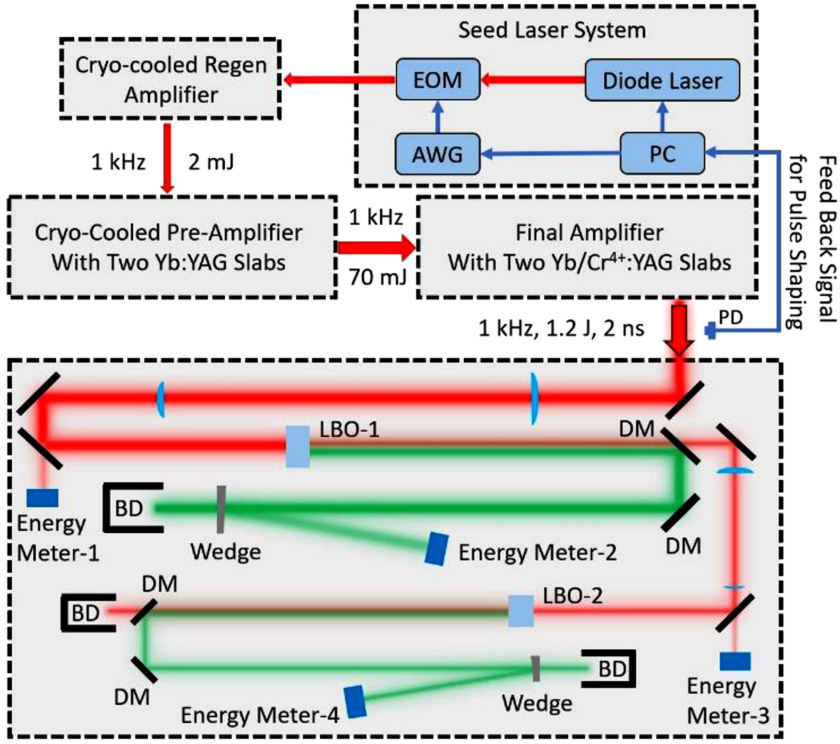

Figure 1.19. Schematic of the high average power, 1 J, green laser setup. The high power $\lambda = 515$ nm laser system includes a seed pulse laser front-end that generates pulses of arbitrary shape, a chain of diode-pumped Yb:YAG cryogenic amplifiers, and two sequentially placed LBO SHG units. DM, dichroic mirror; BD, beam dumper; PD, photodiode. Reprinted with permission from Chi *et al* [60] © The Optical Society.

that described above has been frequency-doubled in LBO to generate 1 J green pulses and 1 kW average power [60].

This frequency-doubled Yb:YAG laser is schematically illustrated in figure 1.19. Infrared laser pulses of 1.2 J energy are produced with 1.2 kW average power and are frequency-doubled in two LBO crystals. Temporally square pulses were generated to maintain the intensity impinging into the doubling crystals at the optimum value for frequency doubling. Because the temporal profile of the pulses injected into the amplifier chain is re-shaped by gain saturation as they are amplified to the Joule level, the seed pulses are generated by an arbitrary-waveform laser, which is programmable to generate a square pulse shape at the end of the amplifier chain. A schematic of the setup used to generate seed pulses of arbitrary shape is shown in the upper part of figure 1.19. The seed laser comprises a 2 W peak power $\lambda = 1030$ nm diode laser, an electro-optic modulator (EOM), an arbitrary-waveform generator (AWG), and a processing unit. The seed semiconductor laser is temperature tuned to operate at the wavelength corresponding to high gain in the following chain of Yb:YAG cryogenic amplifiers. A photodiode is placed at the output of the amplifier chain to monitor the final pulse shape and provide the feedback necessary

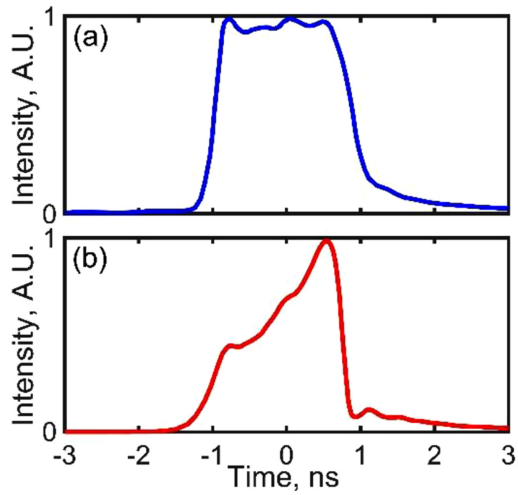

Figure 1.20. Temporal profiles of the (a) output pulse from the final amplifier, and (b) the seed pulse measured before the regenerative amplifier. Reprinted with permission from Chi *et al* [60] © The Optical Society.

to adjust the input signal of the programmable AWG. The adjusted signal is then again applied to the EOM. This feedback process repeats until the desired pulse shape is achieved at the output of the amplifier chain. Figure 1.20(a) shows the measured temporal profile of the amplified 1.2 J square pulse, along with that corresponding to the shaped seed pulse before the cryogenically-cooled regenerative amplifier (figure 1.20(b)). While only the square pulse shape relevant to SHG is presented here, other pulse shapes can be generated with the same setup for other applications.

The shaped seed pulses were amplified to an energy of >1.2 J at 1 kHz repetition rate by a chain of cryogenically-cooled Yb:YAG amplifiers similar to that described above, but in which the regenerative amplifier stage is also cryogenically cooled. LBO crystals cut at $\theta = 90°$ and $\phi = 13.6°$ for Type-I phase matching were placed at the output of the final amplification stage for upconversion into $\lambda = 515$ nm laser light. To make the most efficient use of the fundamental beam, two LBO crystals mounted on temperature-controlled copper holders at 300 K were set up in series as shown in figure 1.19. A Keplerian telescope was used to image the output of the Yb:YAG amplifier chain with selected demagnification onto the first LBO crystal (13 mm thick). The second-harmonic beam was separated from the fundamental by a sequence of two dichroic mirrors. The unconverted $\lambda = 1030$ nm beam was imaged into a second LBO crystal. Figure 1.21 shows the $\lambda = 515$ nm laser pulse energy and SHG conversion efficiency as a function of the $\lambda = 1030$ nm pulse energy obtained with the 13-mm-thick LBO crystal for a 14 mm diameter beam with a fluence of up to 0.78 J cm^{-2}. The pulse energy reaches 0.94 J, corresponding to an average power of 940 W with a shot-to-shot standard deviation of 2.9% and a conversion efficiency of 78%. The unconverted beam was upconverted in the second LBO crystal, which generated additional >100 mJ pulses at $\lambda = 515$ nm. The resulting total $\lambda = 515$ nm average power reaches 1.04 kW (1.04 J pulses at 1 kHz repetition rate).

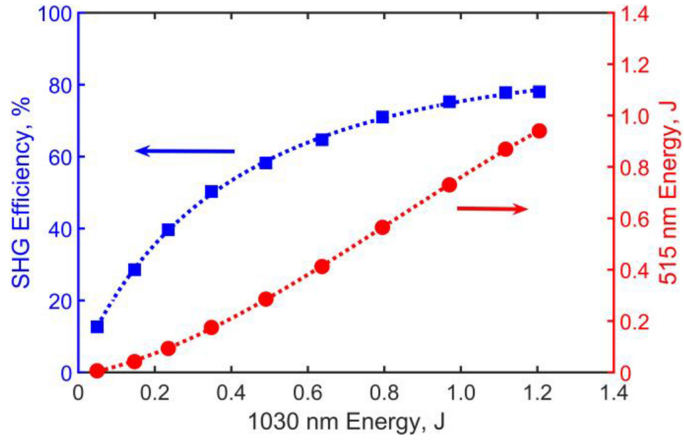

Figure 1.21. SHG efficiency (blue) and SHG output energy (red) vs. fundamental pulse energy obtained with a 13-mm-thick LBO crystal at 1 kHz repetition rate. Reprinted with permission from Chi *et al* [60] © The Optical Society.

Figures 1.22(a) and (b) show that both the $\lambda = 515$ nm, 0.94 J and the secondary 100 mJ beams display flat-top profiles with good uniformity. The second-harmonic beam is characterized by a measured $M^2 = 1.40$ and 1.32 on the horizontal and vertical directions, respectively (figure 1.22(c)).

An even higher conversion efficiency of 89% was obtained with a 10-mm-thick LBO crystal when 0.65 J fundamental wavelength pulses were downsized to achieve a fluence of 0.83 J cm^{-2}, as shown in figure 1.23.

These SHG results will enable the generation of high energy laser pulses of femtosecond duration at 1 kHz repetition rate. In addition, the generation of Joule-level nanosecond pulses of arbitrary shape from a kW average power Yb:YAG laser system will benefit other applications such as heating tailored plasmas for extreme ultraviolet light generation.

1.5 Status and prospects

Yb:YAG picosecond lasers have already reached a pulse energy of 1 J at a repetition rate of 1 kHz. Further increases in both the average power and the pulse energy are expected. Yb:YAG is a mature, thoroughly studied material that is broadly available with high optical quality. It has the advantages of relatively long upper level lifetime that allows for efficient pumping with commercial high power laser diodes. It also has high thermal conductivity and small quantum defect, both of which ease the challenges of thermal management. In addition, Yb:YAG has a relatively broad spectral bandwidth that allows for the generation of picosecond pulses using chirped pulse amplification. These properties that make Yb:YAG attractive for the development of high average power, high energy ultrashort pulse lasers, further improve at cryogenic temperatures. When used in an active mirror geometry either in a thin disk geometry or in thicker gain medium geometries at cryogenic temperature, Yb:YAG enables the generation of Joule-level output pulses at record average powers. Compressed pulses of

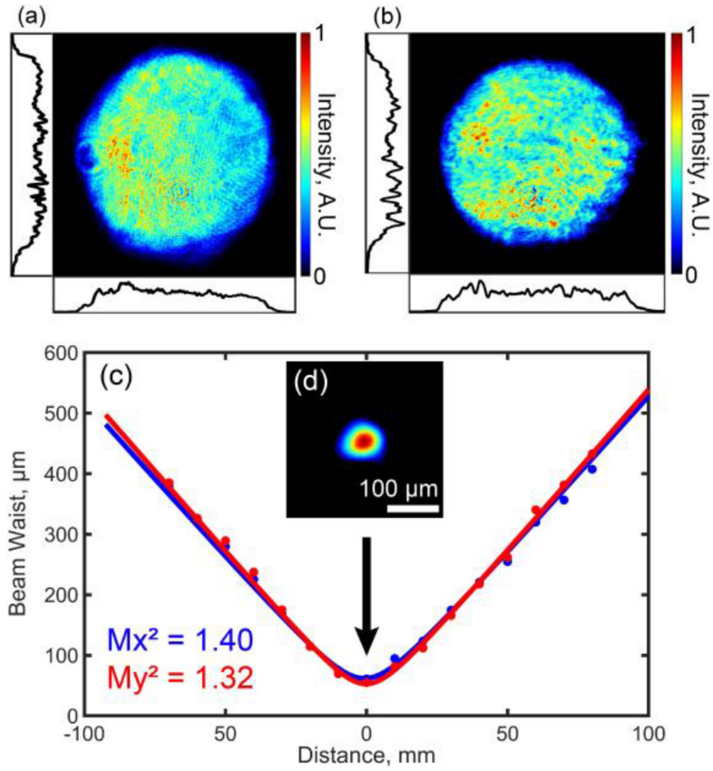

Figure 1.22. Intensity profiles of the $\lambda = 515$ nm beams of pulse energy (a) 0.94 J, and (b) 100 mJ at 1 kHz repetition rate; (c) M^2 measurement of the $\lambda = 515$ nm primary beam, and (d) beam profile at the focal spot. Reprinted with permission from Chi *et al* [60] © The Optical Society.

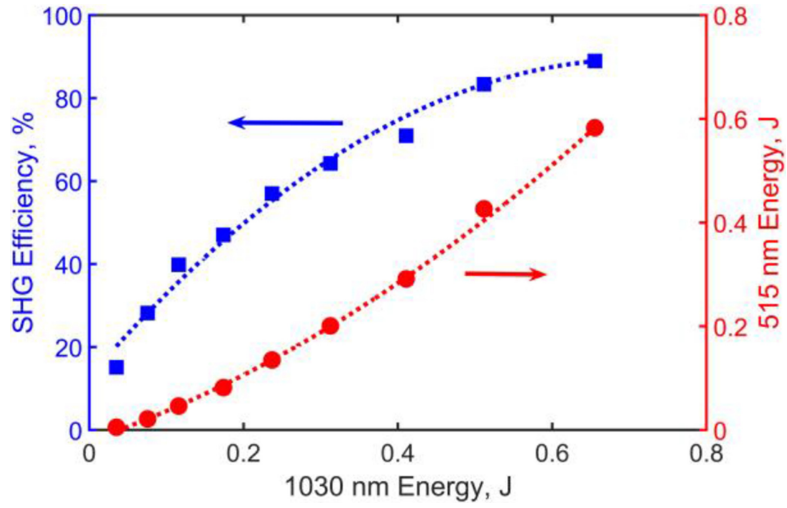

Figure 1.23. SHG efficiency (blue) and SHG output energy (red) vs. fundamental energy obtained with a 10-mm-thick LBO crystal at 1 kHz repetition rate. Reprinted with permission from Chi *et al* [60] © The Optical Society.

720 mJ energy and 0.92 ps duration at 1 kHz repetition rate have been reported for a laser based on thin disks. A laser system based on cryogenically-cooled Yb:YAG has produced 1.1 J pulses of 4.5 ps duration at a 1 kHz repetition rate, an average power of 1.1 kW, which is a record for Joule-level picosecond lasers. These Joule-level high repetition rate lasers have already been used in applications that include pumping plasma-based soft x-ray lasers and producing filaments in the atmosphere to guide lightning. Future trends include the further increase in both the average power and the pulse energy, and the reduction of the pulse duration. Multi-Joule outputs at several kHz can be expected. Finally, while the pulse duration of these lasers has been bandwidth limited to about 1 ps, techniques for spectral broadening of high energy pulses are feasible and offer a path to femtosecond operation [61].

References

[1] Danson C N *et al* 2019 Petawatt and exawatt class lasers worldwide *High Power Laser Sci. Eng.* **7** 54

[2] Moses E I, Boyd R N, Remington B A, Keane C J and Al-Ayat R 2009 The National Ignition Facility: ushering in a new age for high energy density science *Phys. Plasmas* **16** 13

[3] Kawanaka J, Yamakawa K, Nishioka H and Ueda K 2003 30-mJ, diode-pumped, chirped-pulse Yb:YLF regenerative amplifier *Opt. Lett.* **28** 2121–23

[4] Hong K H, Gopinath J T, Rand D, Siddiqui A M, Huang S W, Li E, Eggleton B J, Hybl J D, Fan T Y and Kartner F X 2010 High-energy, kHz-repetition-rate, ps cryogenic Yb:YAG chirped-pulse amplifier *Opt. Lett.* **35** 1752–54

[5] Papadopoulos D N, Pellegrina A, Ramirez L P, Georges P and Druon F 2011 Broadband high-energy diode-pumped Yb:KYW multipass amplifier *Opt. Lett.* **36** 3816–18

[6] Tummler J, Jung R, Stiel H, Nickles P V and Sandner W 2009 High-repetition-rate chirped-pulse-amplification thin-disk laser system with joule-level pulse energy *Opt. Lett.* **34** 1378–80

[7] Jung R, Tummler J, Nubbemeyer T and Will I 2016 Thin-disk ring amplifier for high pulse energy *Opt. Express* **24** 4375–81

[8] Zapata L E, Lin H, Calendron A L, Cankaya H, Hemmer M, Reichert F, Huang W R, Granados E, Hong K H and Kartner F X 2015 Cryogenic Yb:YAG composite-thin-disk for high energy and average power amplifiers *Opt. Lett.* **40** 2610–13

[9] Chang C L *et al* 2015 High-energy, kHz, picosecond hybrid Yb-doped chirped-pulse amplifier *Opt. Express* **23** 10132–44

[10] Metzger T, Schwarz A, Teisset C Y, Sutter D, Killi A, Kienberger R and Krausz F 2009 High-repetition-rate picosecond pump laser based on a Yb:YAG disk amplifier for optical parametric amplification *Opt. Lett.* **34** 2123–25

[11] Fattahi H, Alismail A, Wang H C, Brons J, Pronin O, Buberl T, Vamos L, Arisholm G, Azzeer A M and Krausz F 2016 High-power, 1-ps, all-Yb:YAG thin-disk regenerative amplifier *Opt. Lett.* **41** 1126–29

[12] Rand D A *et al* 2011 Picosecond pulses from a cryogenically cooled, composite amplifier using Yb:YAG and Yb:GSAG *Opt. Lett.* **36** 340–42

[13] Miller D E, Zapata L E, Ripin D J and Fan T Y 2012 Sub-picosecond pulses at 100 W average power from a Yb:YLF chirped-pulse amplification system *Opt. Lett.* **37** 2700–2

[14] Novak J *et al* 2016 Thin disk amplifier-based 40 mJ, 1 kHz, picosecond laser at 515 nm *Opt. Express* **24** 5728–33

[15] Fischer J, Heinrich A C, Maier S, Jungwirth J, Brida D and Leitenstorfer A 2016 615 fs pulses with 17 mJ energy generated by an Yb:thin-disk amplifier at 3 kHz repetition rate *Opt. Lett.* **41** 246–49
[16] Nubbemeyer T *et al* 2017 1 kW, 200 mJ picosecond thin-disk laser system *Opt. Lett.* **42** 1381–84
[17] Klingebiel S, Wandt C, Skrobol C, Ahmad I, Trushin S A, Major Z, Krausz F and Karsch S 2011 High energy picosecond Yb:YAG CPA system at 10 Hz repetition rate for pumping optical parametric amplifiers *Opt. Express* **19** 5357–63
[18] Morrissey F X, Fan T Y, Miller D E and Rand D 2017 Picosecond kilohertz-class cryogenically cooled multistage Yb-doped chirped pulse amplifier *Opt. Lett.* **42** 707–10
[19] Schmidt B E, Hage A, Mans T, Legare F and Woerner H J 2017 Highly stable, 54 mJ Yb-InnoSlab laser platform at 0.5 kW average power *Opt. Express* **25** 17549–55
[20] Herkommer C *et al* 2020 Ultrafast thin-disk multipass amplifier with 720 mJ operating at kilohertz repetition rate for applications in atmospheric research *Opt. Express* **28** 30164–73
[21] Furch F J, Reagan B A, Luther B M, Curtis A H, Meehan S P and Rocca J J 2009 Demonstration of an all-diode-pumped soft x-ray laser *Opt. Lett.* **34** 3352–54
[22] Reagan B A *et al* 2014 1 Joule, 100 Hz repetition rate, picosecond CPA laser for driving high average power soft x-ray lasers *Conf. on Lasers and Electro-Optics (CLEO)* (San Jose, CA: IEEE)
[23] Baumgarten C, Pedicone M, Bravo H, Wang H C, Yin L, Menoni C S, Rocca J J and Reagan B A 2016 1 J, 0.5 kHz repetition rate picosecond laser *Opt. Lett.* **41** 3339–42
[24] Curtis A H, Reagan B A, Wernsing K A, Furch F J, Luther B M and Rocca J J 2011 Demonstration of a compact 100 Hz, 0.1 J, diode-pumped picosecond laser *Opt. Lett.* **36** 2164–66
[25] Zapata L E, Schweisthal S, Thesinga J, Zapata C, Schust M, Yizhou L, Calendron A-L, Pergament M and Kaertner F X 2019 Joule-class 500 Hz cryogenic Yb:YAG chirped pulse amplifier *Conf. on Lasers and Electro-Optics Europe and European Quantum Electronics Conf. 2019* (Munich: Optical Society of America)
[26] Wang Y, Chi H, Baumgarten C, Dehne K, Meadows A R, Davenport A, Murray G, Reagan B A, Menoni C S and Rocca J J 2020 1.1 J Yb:YAG picosecond laser at 1 kHz repetition rate *Opt. Lett.* **45** 6615–18
[27] Chenais S, Druon F, Forget S, Balembois F and Georges P 2006 On thermal effects in solid-state lasers: the case of ytterbium-doped materials *Prog. Quantum Electron.* **30** 89–153
[28] Aggarwal R L, Ripin D J, Ochoa J R and Fan T Y 2005 Measurement of thermo-optic properties of $Y_3Al_5O_{12}$, $Lu_3Al_5O_{12}$, YAIO(3), $LiYF_4$, $LiLuF_4$, BaY_2F_8, KGd(WO_4)(2), and KY(WO_4)(2) laser crystals in the 80–300 K temperature range *J. Appl. Phys.* **98** 14
[29] Calendron A L, Cankaya H and Kartner F X 2014 High-energy kHz Yb:KYW dual-crystal regenerative amplifier *Opt. Express* **22** 24752–62
[30] Siebold M, Bock S, Schramm U, Xu B, Doualan J L, Camy P and Moncorge R 2009 Yb: CaF2—a new old laser crystal *Appl. Phys.* B **97** 327–38
[31] Kuleshov N V, Lagatsky A A, Podlipensky A V, Mikhailov V P and Huber G 1997 Pulsed laser operation of Yb-doped KY(WO_4)(2) and KGd(WO_4)(2) *Opt. Lett.* **22** 1317–19
[32] Koechner W 2006 *Solid State Laser Engineering* (Berlin: Springer)
[33] Ogawa K, Akahane Y, Aoyama M, Tsuji K, Tokita S, Kawanaka J, Nishioka H and Yamakawa K 2007 Multi-millijoule, diode-pumped, cryogenically-cooled Yb:KY(WO_4)(2) chirped-pulse regenerative amplifier *Opt. Express* **15** 8598–602

[34] Liu H H, Nees J and Mourou G 2002 Directly diode-pumped Yb:KY(WO_4)(2) regenerative amplifiers *Opt. Lett.* **27** 722–24
[35] Caracciolo E, Kemnitzer M, Guandalini A, Pirzio F, Agnesi A and Au J A D 2014 High pulse energy multiwatt Yb:$CaAlGdO_4$ and Yb:CaF_2 regenerative amplifiers *Opt. Express* **22** 19912–18
[36] Fan T Y, Ripin D J, Aggarwal R L, Ochoa J R, Chann B, Tilleman M and Spitzberg J 2007 Cryogenic Yb^{3+}-doped solid-state lasers *IEEE J. Sel. Top. Quantum Electron.* **13** 448–59
[37] Machinet G *et al* 2013 High-brightness fiber laser-pumped 68 fs-2.3 W Kerr-lens mode-locked Yb:CaF_2 oscillator *Opt. Lett.* **38** 4008–10
[38] Pugzlys A *et al* 2009 Multi-mJ, 200-fs, cw-pumped, cryogenically cooled, Yb,Na:CaF_2 amplifier *Opt. Lett.* **34** 2075–77
[39] Albach D, Loeser M, Siebold M and Schramm U 2019 Performance demonstration of the PENELOPE main amplifier HEPA I using broadband nanosecond pulses *High Power Laser Sci. Eng.* **7** 9
[40] Hornung M *et al* 2016 54 J pulses with 18 nm bandwidth from a diode-pumped chirped-pulse amplification laser system *Opt. Lett.* **41** 5413–16
[41] Brunner F *et al* 2002 240-fs pulses with 22-W average power from a mode-locked thin-disk Yb:KY(WO_4)(2) laser *Opt. Lett.* **27** 1162–64
[42] Brunner F *et al* 2000 Diode-pumped femtosecond Yb:KGd(WO_4)(2) laser with 1.1-W average power *Opt. Lett.* **25** 1119–21
[43] Geusic J E, Marcos H M and Vanuitert L G 1964 Laser oscillations in Nd-doped yttrium aluminum yttrium gallium + gadolinium garnets (continuous operation of $Y_3A1_5O_{12}$, pulsed operation of $Y_3Ga_5O_{15}$ + $Gd_3Ga_5O_{12}$ rm temperature) *Appl. Phys. Lett.* **4**(10) 182
[44] Russbueldt P, Mans T, Weitenberg J, Hoffmann H D and Poprawe R 2010 Compact diode-pumped 1.1 kW Yb:YAG Innoslab femtosecond amplifier *Opt. Lett.* **35** 4169–71
[45] Wynne R, Daneu J L and Fan T Y 1999 Thermal coefficients of the expansion and refractive index in YAG *Appl. Opt.* **38** 3282–84
[46] Dong J, Bass M, Mao Y L, Deng P Z and Gan F X 2003 Dependence of the Yb^{3+} emission cross section and lifetime on temperature and concentration in yttrium aluminum garnet *J. Opt. Soc. Am.* B **20** 1975–79
[47] Slack G A and Oliver D W 1971 Thermal conductivity of garnets and phonon scattering by rare-earth ions *Phys. Rev.* B **4** 592
[48] Liu Y, Demirbas U, Kellert M, Thesinga J, Cankaya H, Hua Y, Zapata L E, Pergament M and Kärtner F X 2020 Eight-pass Yb:YLF cryogenic amplifier generating 305-mJ pulses *OSA Continuum* **3** 2722–29
[49] Giesen A, Hugel H, Voss A, Wittig K, Brauch U and Opower H 1994 Scalable concept for diode-pumped high-power solid-state lasers *Appl. Phys.* B **58** 365–72
[50] Giesen A and Speiser J 2007 Fifteen years of work on thin-disk lasers: results and scaling laws *IEEE J. Sel. Top. Quantum Electron.* **13** 598–609
[51] Saraceno C J, Sutter D, Metzger T and Ahmed M A 2019 The amazing progress of high-power ultrafast thin-disk lasers *J. Eur. Opt. Soc. Rapid Publ.* **15** 7
[52] Jung R, Tummler J and Will I 2016 Regenerative thin-disk amplifier for 300 mJ pulse energy *Opt. Express* **24** 883–87
[53] Reagan B A, Curtis A H, Wernsing K A, Furch F J, Luther B M and Rocca J J 2012 Development of high energy diode-pumped thick-disk Yb:YAG chirped-pulse-amplification lasers *IEEE J. Quantum Electron.* **48** 827–35

[54] Reagan B A *et al* 2018 Scaling diode-pumped, high energy picosecond lasers to kilowatt average powers *High Power Laser Sci. Eng.* **6** e11

[55] Chi H, Dehne K A, Baumgarten C M, Wang H C, Yin L, Reagan B A and Rocca J J 2018 In situ 3-D temperature mapping of high average power cryogenic laser amplifiers *Opt. Express* **26** 5240–52

[56] Gronloh B, Russbueldt P, Schneider W, Jungbluth B and Hoffmann H D 2012 High average power sub-picosecond pulse generation at 515 nm by extracavity frequency doubling of a mode-locked Innoslab MOPA *Conf. on Solid State Lasers XXI—Technology and Devices* (San Francisco, CA: SPIE—The International Society for Optical Engineering)

[57] Rocker C, Loescher A, Bienert F, Villeval P, Lupinski D, Bauer D, Killi A, Graf T and Ahmed M A 2020 Ultrafast green thin-disk laser exceeding 1.4 kW of average power *Opt. Lett.* **45** 5522–25

[58] Phillips J P *et al* 2016 High energy, high repetition rate, second harmonic generation in large aperture DKDP, YCOB, and LBO crystals *Opt. Express* **24** 19682–94

[59] Bayramian A J *et al* 2009 High average power petawatt laser pumped by the Mercury laser for fusion materials engineering *Fusion Sci. Technol.* **56** 295–300

[60] Chi H, Wang Y, Davenport A, Menoni C S and Rocca J J 2020 Demonstration of a kilowatt average power, 1 J, green laser *Opt. Lett.* **45** 6803–6

[61] Fan G, Carpeggiani P A, Tao Z, Coccia G, Safaei R, Kaksis E, Pugzlys A, Légaré F, Schmidt B E and Baltuška A 2021 70 mJ nonlinear compression and scaling route for an Yb amplifier using large-core hollow fibers *Opt. Lett.* **46** 896–99

Full list of references

Prelims

[1] Strickland D and Mourou G 1985 Compression of amplified chirped optical pulses *Opt. Commun.* **55** 447–9

[2] Doria D *et al* 2020 Overview of ELI-NP status and laser commissioning experiments with 1 PW and 10 PW class-lasers *J. Instrum.* **15** C0903

[3] Yoon J W *et al* 2019 Achieving the laser intensity of 5.5 × 1022 W cm^{-2} with a wavefront-corrected multi-PW laser *Opt. Express* **17** 20413

[4] Danson C N *et al* 2019 Petawatt and exawatt lasers worldwide *High Power Laser Sci. Eng.* **7** e54

[5] Nisoli M *et al* 1996 Generation of high energy 10 fs pulses by a new pulse compression technique *Appl. Phys. Lett.* **68** 2793

[6] Mironov S Y *et al* 2020 Thin plate compression of a sub-petawatt Ti:Sa laser pulses *Appl. Phys. Lett.* **116** 241101

[7] Drescher M *et al* 2001 X-ray pulses approaching the attosecond frontier *Science* **291** 1923–7

[8] Hentschel M *et al* 2001 Attosecond metrology *Nature* **414** 509–13

[9] Krausz F and Ivanov M 2009 Attosecond physics *Rev. Mod. Phys.* **81** 163–234

[10] Young L *et al* 2018 Roadmap of ultrafast X-ray atomic and molecular physics *J. Phys. B: At. Mol. Opt. Phys* **51** 032003

Chapter 1

[1] Danson C N *et al* 2019 Petawatt and exawatt class lasers worldwide *High Power Laser Sci. Eng.* **7** 54

[2] Moses E I, Boyd R N, Remington B A, Keane C J and Al-Ayat R 2009 The National Ignition Facility: ushering in a new age for high energy density science *Phys. Plasmas* **16** 13

[3] Kawanaka J, Yamakawa K, Nishioka H and Ueda K 2003 30-mJ, diode-pumped, chirped-pulse Yb:YLF regenerative amplifier *Opt. Lett.* **28** 2121–23

[4] Hong K H, Gopinath J T, Rand D, Siddiqui A M, Huang S W, Li E, Eggleton B J, Hybl J D, Fan T Y and Kartner F X 2010 High-energy, kHz-repetition-rate, ps cryogenic Yb:YAG chirped-pulse amplifier *Opt. Lett.* **35** 1752–54

[5] Papadopoulos D N, Pellegrina A, Ramirez L P, Georges P and Druon F 2011 Broadband high-energy diode-pumped Yb:KYW multipass amplifier *Opt. Lett.* **36** 3816–18

[6] Tummler J, Jung R, Stiel H, Nickles P V and Sandner W 2009 High-repetition-rate chirped-pulse-amplification thin-disk laser system with joule-level pulse energy *Opt. Lett.* **34** 1378–80

[7] Jung R, Tummler J, Nubbemeyer T and Will I 2016 Thin-disk ring amplifier for high pulse energy *Opt. Express* **24** 4375–81

[8] Zapata L E, Lin H, Calendron A L, Cankaya H, Hemmer M, Reichert F, Huang W R, Granados E, Hong K H and Kartner F X 2015 Cryogenic Yb:YAG composite-thin-disk for high energy and average power amplifiers *Opt. Lett.* **40** 2610–13

[9] Chang C L *et al* 2015 High-energy, kHz, picosecond hybrid Yb-doped chirped-pulse amplifier *Opt. Express* **23** 10132–44

[10] Metzger T, Schwarz A, Teisset C Y, Sutter D, Killi A, Kienberger R and Krausz F 2009 High-repetition-rate picosecond pump laser based on a Yb:YAG disk amplifier for optical parametric amplification *Opt. Lett.* **34** 2123–25

[11] Fattahi H, Alismail A, Wang H C, Brons J, Pronin O, Buberl T, Vamos L, Arisholm G, Azzeer A M and Krausz F 2016 High-power, 1-ps, all-Yb:YAG thin-disk regenerative amplifier *Opt. Lett.* **41** 1126–29

[12] Rand D A *et al* 2011 Picosecond pulses from a cryogenically cooled, composite amplifier using Yb:YAG and Yb:GSAG *Opt. Lett.* **36** 340–42

[13] Miller D E, Zapata L E, Ripin D J and Fan T Y 2012 Sub-picosecond pulses at 100 W average power from a Yb:YLF chirped-pulse amplification system *Opt. Lett.* **37** 2700–2

[14] Novak J *et al* 2016 Thin disk amplifier-based 40 mJ, 1 kHz, picosecond laser at 515 nm *Opt. Express* **24** 5728–33

[15] Fischer J, Heinrich A C, Maier S, Jungwirth J, Brida D and Leitenstorfer A 2016 615 fs pulses with 17 mJ energy generated by an Yb:thin-disk amplifier at 3 kHz repetition rate *Opt. Lett.* **41** 246–49

[16] Nubbemeyer T *et al* 2017 1 kW, 200 mJ picosecond thin-disk laser system *Opt. Lett.* **42** 1381–84

[17] Klingebiel S, Wandt C, Skrobol C, Ahmad I, Trushin S A, Major Z, Krausz F and Karsch S 2011 High energy picosecond Yb:YAG CPA system at 10 Hz repetition rate for pumping optical parametric amplifiers *Opt. Express* **19** 5357–63

[18] Morrissey F X, Fan T Y, Miller D E and Rand D 2017 Picosecond kilohertz-class cryogenically cooled multistage Yb-doped chirped pulse amplifier *Opt. Lett.* **42** 707–10

[19] Schmidt B E, Hage A, Mans T, Legare F and Woerner H J 2017 Highly stable, 54 mJ Yb-InnoSlab laser platform at 0.5 kW average power *Opt. Express* **25** 17549–55

[20] Herkommer C *et al* 2020 Ultrafast thin-disk multipass amplifier with 720 mJ operating at kilohertz repetition rate for applications in atmospheric research *Opt. Express* **28** 30164–73

[21] Furch F J, Reagan B A, Luther B M, Curtis A H, Meehan S P and Rocca J J 2009 Demonstration of an all-diode-pumped soft x-ray laser *Opt. Lett.* **34** 3352–54

[22] Reagan B A *et al* 2014 1 Joule, 100 Hz repetition rate, picosecond CPA laser for driving high average power soft x-ray lasers *Conf. on Lasers and Electro-Optics (CLEO)* (San Jose, CA: IEEE)

[23] Baumgarten C, Pedicone M, Bravo H, Wang H C, Yin L, Menoni C S, Rocca J J and Reagan B A 2016 1 J, 0.5 kHz repetition rate picosecond laser *Opt. Lett.* **41** 3339–42

[24] Curtis A H, Reagan B A, Wernsing K A, Furch F J, Luther B M and Rocca J J 2011 Demonstration of a compact 100 Hz, 0.1 J, diode-pumped picosecond laser *Opt. Lett.* **36** 2164–66

[25] Zapata L E, Schweisthal S, Thesinga J, Zapata C, Schust M, Yizhou L, Calendron A-L, Pergament M and Kaertner F X 2019 Joule-class 500 Hz cryogenic Yb:YAG chirped pulse amplifier *Conf. on Lasers and Electro-Optics Europe and European Quantum Electronics Conf. 2019* (Munich: Optical Society of America)

[26] Wang Y, Chi H, Baumgarten C, Dehne K, Meadows A R, Davenport A, Murray G, Reagan B A, Menoni C S and Rocca J J 2020 1.1 J Yb:YAG picosecond laser at 1 kHz repetition rate *Opt. Lett.* **45** 6615–18

[27] Chenais S, Druon F, Forget S, Balembois F and Georges P 2006 On thermal effects in solid-state lasers: the case of ytterbium-doped materials *Prog. Quantum Electron.* **30** 89–153

[28] Aggarwal R L, Ripin D J, Ochoa J R and Fan T Y 2005 Measurement of thermo-optic properties of $Y_3Al_5O_{12}$, $Lu_3Al_5O_{12}$, YAIO(3), $LiYF_4$, $LiLuF_4$, BaY_2F_8, $KGd(WO_4)(2)$, and $KY(WO_4)(2)$ laser crystals in the 80–300 K temperature range *J. Appl. Phys.* **98** 14

[29] Calendron A L, Cankaya H and Kartner F X 2014 High-energy kHz Yb:KYW dual-crystal regenerative amplifier *Opt. Express* **22** 24752–62
[30] Siebold M, Bock S, Schramm U, Xu B, Doualan J L, Camy P and Moncorge R 2009 Yb: CaF2—a new old laser crystal *Appl. Phys.* B **97** 327–38
[31] Kuleshov N V, Lagatsky A A, Podlipensky A V, Mikhailov V P and Huber G 1997 Pulsed laser operation of Yb-doped $KY(WO_4)(2)$ and $KGd(WO_4)(2)$ *Opt. Lett.* **22** 1317–19
[32] Koechner W 2006 *Solid State Laser Engineering* (Berlin: Springer)
[33] Ogawa K, Akahane Y, Aoyama M, Tsuji K, Tokita S, Kawanaka J, Nishioka H and Yamakawa K 2007 Multi-millijoule, diode-pumped, cryogenically-cooled $Yb:KY(WO_4)(2)$ chirped-pulse regenerative amplifier *Opt. Express* **15** 8598–602
[34] Liu H H, Nees J and Mourou G 2002 Directly diode-pumped $Yb:KY(WO_4)(2)$ regenerative amplifiers *Opt. Lett.* **27** 722–24
[35] Caracciolo E, Kemnitzer M, Guandalini A, Pirzio F, Agnesi A and Au J A D 2014 High pulse energy multiwatt $Yb:CaAlGdO_4$ and $Yb:CaF_2$ regenerative amplifiers *Opt. Express* **22** 19912–18
[36] Fan T Y, Ripin D J, Aggarwal R L, Ochoa J R, Chann B, Tilleman M and Spitzberg J 2007 Cryogenic Yb^{3+}-doped solid-state lasers *IEEE J. Sel. Top. Quantum Electron.* **13** 448–59
[37] Machinet G *et al* 2013 High-brightness fiber laser-pumped 68 fs-2.3 W Kerr-lens mode-locked $Yb:CaF_2$ oscillator *Opt. Lett.* **38** 4008–10
[38] Pugzlys A *et al* 2009 Multi-mJ, 200-fs, cw-pumped, cryogenically cooled, $Yb,Na:CaF_2$ amplifier *Opt. Lett.* **34** 2075–77
[39] Albach D, Loeser M, Siebold M and Schramm U 2019 Performance demonstration of the PENELOPE main amplifier HEPA I using broadband nanosecond pulses *High Power Laser Sci. Eng.* **7** 9
[40] Hornung M *et al* 2016 54 J pulses with 18 nm bandwidth from a diode-pumped chirped-pulse amplification laser system *Opt. Lett.* **41** 5413–16
[41] Brunner F *et al* 2002 240-fs pulses with 22-W average power from a mode-locked thin-disk $Yb:KY(WO_4)(2)$ laser *Opt. Lett.* **27** 1162–64
[42] Brunner F *et al* 2000 Diode-pumped femtosecond $Yb:KGd(WO_4)(2)$ laser with 1.1-W average power *Opt. Lett.* **25** 1119–21
[43] Geusic J E, Marcos H M and Vanuitert L G 1964 Laser oscillations in Nd-doped yttrium aluminum yttrium gallium + gadolinium garnets (continuous operation of $Y_3A1_5O_{12}$, pulsed operation of $Y_3Ga_5O_{15}$ + $Gd_3Ga_5O_{12}$ rm temperature) *Appl. Phys. Lett.* **4**(10) 182
[44] Russbueldt P, Mans T, Weitenberg J, Hoffmann H D and Poprawe R 2010 Compact diode-pumped 1.1 kW Yb:YAG Innoslab femtosecond amplifier *Opt. Lett.* **35** 4169–71
[45] Wynne R, Daneu J L and Fan T Y 1999 Thermal coefficients of the expansion and refractive index in YAG *Appl. Opt.* **38** 3282–84
[46] Dong J, Bass M, Mao Y L, Deng P Z and Gan F X 2003 Dependence of the Yb^{3+} emission cross section and lifetime on temperature and concentration in yttrium aluminum garnet *J. Opt. Soc. Am.* B **20** 1975–79
[47] Slack G A and Oliver D W 1971 Thermal conductivity of garnets and phonon scattering by rare-earth ions *Phys. Rev.* B **4** 592
[48] Liu Y, Demirbas U, Kellert M, Thesinga J, Cankaya H, Hua Y, Zapata L E, Pergament M and Kärtner F X 2020 Eight-pass Yb:YLF cryogenic amplifier generating 305-mJ pulses *OSA Continuum* **3** 2722–29

[49] Giesen A, Hugel H, Voss A, Wittig K, Brauch U and Opower H 1994 Scalable concept for diode-pumped high-power solid-state lasers *Appl. Phys.* B **58** 365–72
[50] Giesen A and Speiser J 2007 Fifteen years of work on thin-disk lasers: results and scaling laws *IEEE J. Sel. Top. Quantum Electron.* **13** 598–609
[51] Saraceno C J, Sutter D, Metzger T and Ahmed M A 2019 The amazing progress of high-power ultrafast thin-disk lasers *J. Eur. Opt. Soc. Rapid Publ.* **15** 7
[52] Jung R, Tummler J and Will I 2016 Regenerative thin-disk amplifier for 300 mJ pulse energy *Opt. Express* **24** 883–87
[53] Reagan B A, Curtis A H, Wernsing K A, Furch F J, Luther B M and Rocca J J 2012 Development of high energy diode-pumped thick-disk Yb:YAG chirped-pulse-amplification lasers *IEEE J. Quantum Electron.* **48** 827–35
[54] Reagan B A *et al* 2018 Scaling diode-pumped, high energy picosecond lasers to kilowatt average powers *High Power Laser Sci. Eng.* **6** e11
[55] Chi H, Dehne K A, Baumgarten C M, Wang H C, Yin L, Reagan B A and Rocca J J 2018 In situ 3-D temperature mapping of high average power cryogenic laser amplifiers *Opt. Express* **26** 5240–52
[56] Gronloh B, Russbueldt P, Schneider W, Jungbluth B and Hoffmann H D 2012 High average power sub-picosecond pulse generation at 515 nm by extracavity frequency doubling of a mode-locked Innoslab MOPA *Conf. on Solid State Lasers XXI—Technology and Devices* (San Francisco, CA: SPIE—The International Society for Optical Engineering)
[57] Rocker C, Loescher A, Bienert F, Villeval P, Lupinski D, Bauer D, Killi A, Graf T and Ahmed M A 2020 Ultrafast green thin-disk laser exceeding 1.4 kW of average power *Opt. Lett.* **45** 5522–25
[58] Phillips J P *et al* 2016 High energy, high repetition rate, second harmonic generation in large aperture DKDP, YCOB, and LBO crystals *Opt. Express* **24** 19682–94
[59] Bayramian A J *et al* 2009 High average power petawatt laser pumped by the Mercury laser for fusion materials engineering *Fusion Sci. Technol.* **56** 295–300
[60] Chi H, Wang Y, Davenport A, Menoni C S and Rocca J J 2020 Demonstration of a kilowatt average power, 1 J, green laser *Opt. Lett.* **45** 6803–6
[61] Fan G, Carpeggiani P A, Tao Z, Coccia G, Safaei R, Kaksis E, Pugzlys A, Légaré F, Schmidt B E and Baltuška A 2021 70 mJ nonlinear compression and scaling route for an Yb amplifier using large-core hollow fibers *Opt. Lett.* **46** 896–99

Chapter 2

[1] Maiman T H 1960 Stimulated optical radiation in ruby *Nature* **187** 493–4
[2] Strickland D and Mourou G 1985 Compression of amplified chirped optical pulses *Opt. Commun.* **56** 219–21
[3] Negel J-P, Loescher A, Voss A, Bauer D, Sutter D, Killi A, Ahmed M A and Graf T 2015 Ultrafast thin-disk multipass laser amplifier delivering 1.4 kW (47 mJ, 1030 nm) average power converted to 820 W at 515 nm and 234 W at 343 nm *Opt. Express* **23** 21064
[4] Nubbemeyer T *et al* 2017 1-kW, 200-mJ, picosecond thin-disk laser system *Opt. Lett.* **42** 1381–4
[5] Russbueldt P, Mans T, Weitenberg J, Hoffmann H D and Poprawe R 2010 Compact diode-pumped 1.1 kW Yb:YAG Innoslab femtosecond amplifier *Opt. Lett.* **35** 4169–71
[6] Jauregui C, Limpert J and Tünnermann A 2013 High-power fibre lasers *Nat. Photonics* **7** 861–7

[7] Zervas M N and Codemard C A 2014 High power fiber lasers: a review *IEEE J. Sel. Top. Quantum Electron.* **20** 219–41
[8] Fried N M 2005 High-power laser vaporization of the canine prostate using a 110 W thulium fiber laser at 1.91 μm *Lasers Surg. Med.* **36** 52–6
[9] Traxer O and Keller E X 2020 Thulium fiber laser: the new player for kidney stone treatment? A comparison with Holmium:YAG laser *World J. Urol.* **38** 1883–94
[10] Mingareev I, Weirauch F, Olowinsky A, Shah L, Kadwani P and Richardson M 2012 Welding of polymers using a 2 μm thulium fiber laser *Opt. Laser Technol.* **44** 2095–9
[11] Pires H, Baudisch M, Sanchez D, Hemmer M and Biegert J 2015 Ultrashort pulse generation in the mid-IR *Prog. Quantum Electron.* **43** 1–30
[12] Shamir Y, Rothhardt J, Hädrich S, Demmler S, Tschernajew M, Limpert J and Tünnermann A 2015 High-average-power 2 μm few-cycle optical parametric chirped pulse amplifier at 100 kHz repetition rate *Opt. Lett.* **40** 5546
[13] Windeler M K R, Mecseki K, Miahnahri A, Robinson J S, Fraser J M, Fry A R and Tavella F 2019 100 W high-repetition-rate near-infrared optical parametric chirped pulse amplifier *Opt. Lett.* **44** 4287
[14] Moulton P F *et al* 2009 Tm-doped fiber lasers: Fundamentals and power scaling *IEEE J. Sel. Top. Quantum Electron.* **15** 85–92
[15] Jackson S D 2004 Cross relaxation and energy transfer upconversion processes relevant to the functioning of 2 μm Tm^{3+}-doped silica fibre lasers *Opt. Commun.* **230** 197–203
[16] Sincore A, Bradford J D, Cook J, Shah L and Richardson M C 2018 High average power thulium-doped silica fiber lasers: review of systems and concepts *IEEE J. Sel. Top. Quantum Electron.* **24** 1–8
[17] Gebhardt M, Gaida C, Stutzki F, Hädrich S, Jauregui C, Limpert J and Tünnermann A 2015 Impact of atmospheric molecular absorption on the temporal and spatial evolution of ultra-short optical pulses *Opt. Express* **23** 13776
[18] Agrawal G P 2006 *Nonlinear Fiber Optics* 3rd edn (New York: Academic)
[19] Jauregui C, Stihler C and Limpert J 2020 Transverse mode instability *Adv. Opt. Photonics* **12** 429
[20] Jackson S D and King T A 1999 Theoretical modeling of Tm-doped silica fiber lasers *J. Lightwave Technol.* **17** 948–56
[21] Peterka P, Faure B, Blanc W, Karásek M and Dussardier B 2004 Theoretical modelling of S-band thulium-doped silica fibre amplifiers *Opt. Quantum Electron.* **36** 201–12
[22] Hanna D C, Perry I R, Lincoln J R and Townsend J E 1990 A 1-Watt thulium-doped cw fibre laser operating at 2 μm *Opt. Commun.* **80** 52–6
[23] Creeden D, Johnson B R, Rines G A and Setzler S D 2014 High power resonant pumping of Tm-doped fiber amplifiers in core- and cladding-pumped configurations *Opt. Express* **22** 29067
[24] Newburgh G A, Zhang J and Dubinskii M 2017 Tm-doped fiber laser resonantly diode-cladding-pumped at 1620 nm *Laser Phys. Lett.* **14** 125101
[25] Creeden D, Johnson B R, Setzler S D and Chicklis E P 2014 Resonantly pumped Tm-doped fiber laser with 90% slope efficiency *Opt. Lett.* **39** 470
[26] Petit V, Carter A, Tumminelli R, Hemming A, Haub J and Simakov N 2018 Highly doped and highly efficient Tm doped fiber laser (conference presentation) *Fiber Lasers XV: Technology and Systems* ed A L Carter and I Hartl (Bellingham, WA: SPIE), p 21

[27] McCumber D E 1964 Einstein relations connecting broadband emission and absorption spectra *Phys. Rev.* **136** A954–7
[28] Milam D 1998 Review and assessment of measured values of the nonlinear refractive-index coefficient of fused silica *Appl. Opt.* **37** 546
[29] Gaida C, Gebhardt M, Stutzki F, Jauregui C, Limpert J and Tünnermann A 2015 Self-compression in a solid fiber to 24 MW peak power with few-cycle pulses at 2 μm wavelength *Opt. Lett.* **40** 5160
[30] Cook J, Bradford J D, Bodnar N, Richardson M C and Sincore A M 2018 Experimental investigation on varying spectral bandwidth when amplifying a pulsed superfluorescent 2-μm source in Tm:fiber *Fiber Lasers XV: Technology and Systems* ed A L Carter and I Hartl (Bellingham, WA: SPIE), p 24
[31] Limpert J, Stutzki F, Jansen F, Otto H-J, Eidam T, Jauregui C and Tünnermann A 2012 Yb-doped large-pitch fibres: effective single-mode operation based on higher-order mode delocalisation *Light: Sci. Appl.* **1** e8
[32] Eidam T, Wirth C, Jauregui C, Stutzki F, Jansen F, Otto H, Schmidt O, Schreiber T, Limpert J and Tünnermann A 2011 Experimental observations of the threshold-like onset of mode instabilities in high power fiber amplifiers *Opt. Express* **19** 13218–24
[33] Otto H-J, Stutzki F, Jansen F, Eidam T, Jauregui C, Limpert J and Tünnerman A 2012 Experimental study of mode instabilities in high power fiber amplifiers *Advanced Solid-State Photonics, ASSP 2012* (Baltimore, MA: Optical Society of America)
[34] Erdogan T 1997 Fiber grating spectra *J. Lightwave Technol.* **15** 1277–94
[35] Arlee J J S, Smith V, Smith A V and Smith J J 2015 Mode instability thresholds for Tm-doped fiber amplifiers pumped at 790 nm *Opt. Express* **2304** 11407–22
[36] Goodno G D, Book L D and Rothenberg J E 2009 Low-phase-noise, single-frequency, single-mode 608 W thulium fiber amplifier *Opt. Lett.* **34** 1204
[37] Gaida C *et al* 2018 Ultrafast thulium fiber laser system emitting more than 1 kW of average power *Opt. Lett.* **43** 5853
[38] Gaida C, Gebhardt M, Heuermann T, Wang Z, Stutzki F, Jauregui-Misas C and Limpert J 2019 Observation of transverse-mode instabilities in a thulium-doped fiber amplifier *Fiber Lasers XVI: Technology and Systems* vol 1089702 ed L Dong and A L Carter (Bellingham, WA: SPIE), p 1
[39] Jansen F, Stutzki F, Jauregui C, Limpert J and Tünnermann A 2012 High-power very large mode-area thulium-doped fiber laser *Opt. Lett.* **37** 4546
[40] Schimpf D N, Eidam T, Seise E, Hädrich S, Limpert J and Tünnermann A 2009 Circular versus linear polarization in laser-amplifiers with Kerr-nonlinearity *Opt. Express* **17** 18774
[41] Imeshev G and Fermann M E 2005 230-kW peak power femtosecond pulses from a high power tunable source based on amplification in Tm-doped fiber *Opt. Express* **13** 7424–31
[42] Haxsen F, Wandt D, Morgner U, Neumann J J and Kracht D 2010 Pulse energy of 151 nJ from ultrafast thulium-doped chirped-pulse fiber amplifier *Opt. Lett.* **35** 2991–3
[43] Sims R A, Kadwani P, Shah A S L and Richardson M 2013 1 μJ, sub-500 fs chirped pulse amplification in a Tm-doped fiber system *Opt. Lett.* **38** 121–3
[44] Wan P, Yang L-M and Liu J 2013 High pulse energy 2 μm femtosecond fiber laser *Opt. Express* **21** 1798–803
[45] Wan P, Yang L and Liu J 2013 156 micro-J ultrafast Thulium-doped fiber laser *Proc. SPIE* **1** 7–13

[46] Stutzki F, Gaida C, Gebhardt M, Jansen F, Jauregui C, Limpert J and Tünnermann A 2015 Tm-based fiber-laser system with more than 200 MW peak power *Opt. Lett.* **40** 9–12
[47] Gaida C, Gebhardt M, Stutzki F, Jauregui C, Limpert J and Tünnermann A 2016 Thulium-doped fiber chirped-pulse amplification system with 2 GW of peak power *Opt. Lett.* **41** 4130
[48] Gaida C, Gebhardt M, Stutzki F, Jauregui C, Limpert J and Tünnermann A 2017 90 fs pulses with >5 GW peak power from a high repetition rate Tm-doped fiber CPA system *Optics InfoBase Conf. Papers* vol Part F75-A
[49] Otto H, Stutzki F, Jansen F, Eidam T, Jauregui C, Limpert J and Tünnermann A 2012 Temporal dynamics of mode instabilities in high-power fiber lasers and amplifiers *Opt. Express* **20** 10180–92
[50] Sims R A, Kadwani P, Ebendorff-Heideprem H, Shah L, Monro T M and Richardson M 2013 Chirped pulse amplification in single mode Tm:fiber using a chirped Bragg grating *Appl. Phys.* B **111** 299–304
[51] Yang L-M, Wan P, Protopopov V and Liu J 2012 2 micron femtosecond fiber laser at low repetition rate and high pulse energy *Opt. Express* **20** 5683–8
[52] Wan P, Yang L-M and Liu J 2013 High power 2 μm femtosecond fiber laser *Opt. Express* **21** 21374
[53] Stutzki F *et al* 2014 152 W average power Tm-doped fiber CPA system *Opt. Lett.* **39** 4671–4
[54] Tan F, Shi H, Sun R, Wang P and Wang P 2016 1 μJ, sub-300 fs pulse generation from a compact thulium-doped chirped pulse amplifier seeded by Raman shifted erbium-doped fiber laser *Opt. Express* **24** 22461
[55] Cossel K C, Waxman E M, Finneran I A, Blake G A, Ye J and Newbury N R 2017 Gas-phase broadband spectroscopy using active sources: progress, status, and applications [Invited] *J. Opt. Soc. Am.* B **34** 104–29
[56] Yang X, Zhao X, Yang K, Liu Y, Liu Y, Fu W and Luo Y 2016 Biomedical applications of terahertz spectroscopy and imaging *Trends Biotechnol.* **34** 810–24
[57] Hafez H A, Chai X, Ibrahim A, Mondal S, Férachou D, Ropagnol X and Ozaki T 2016 Intense terahertz radiation and their applications *J. Opt.* **18** 093004
[58] Redo-Sanchez A, Laman N, Schulkin B and Tongue T 2013 Review of terahertz technology readiness assessment and applications *J. Infrared Millim. Terahertz Waves* **34** 500–18
[59] Le Gros M A, McDermott G, Cinquin B P, Smith E A, Do M, Chao W L, Naulleau P P and Larabell C A 2014 Biological soft x-ray tomography on beamline 2.1 at the advanced light source *J. Synchrotron Radiat.* **21** 1370–7
[60] Fuchs S *et al* 2016 Nanometer resolution optical coherence tomography using broad bandwidth XUV and soft x-ray radiation *Sci. Rep.* **6** 20658
[61] Miao J, Sandberg R L and Song C 2012 Coherent x-ray diffraction imaging *IEEE J. Sel. Top. Quantum Electron.* **18** 399–410
[62] Pertot Y *et al* 2017 Time-resolved x-ray absorption spectroscopy with a water window high-harmonic source *Science* **355** 264
[63] Tisch J W G 2008 Ultrafast goes ultralong *Nat. Phys.* **4** 350–1
[64] Shiner A D, Trallero-Herrero C, Kajumba N, Bandulet H C, Comtois D, Légaré F, Giguère M, Kieffer J C, Corkum P B and Villeneuve D M 2009 Wavelength scaling of high harmonic generation efficiency *Phys. Rev. Lett.* **103** 073902
[65] Haas J and Mizaikoff B 2016 Advances in mid-infrared spectroscopy for chemical analysis *Annu. Rev. Anal. Chem.* **9** 45–68

[66] Henderson B *et al* 2018 Laser spectroscopy for breath analysis: towards clinical implementation *Appl. Phys.* B **124** 161
[67] Griffiths P R and de Haseth J A 2007 *Fourier Transform Infrared Spectrometry* 2nd edn (New York: Wiley) https://doi.org/10.1002/047010631X
[68] Baker M J *et al* 2014 Using Fourier transform IR spectroscopy to analyze biological materials *Nat. Protoc.* **9** 1771
[69] Doherty J, Cinque G and Gardner P 2017 Single-cell analysis using Fourier transform infrared microspectroscopy *Appl. Spectrosc. Rev.* **52** 560–87
[70] Petrov V 2015 Frequency down-conversion of solid-state laser sources to the mid-infrared spectral range using non-oxide nonlinear crystals *Prog. Quantum Electron.* **42** 1–106
[71] Boyd R W 2008 *Nonlinear Optics* 3rd edn (Amsterdam: Elsevier)
[72] Dhillon S S *et al* 2017 The 2017 terahertz science and technology roadmap *J. Phys. D: Appl. Phys.* **50** 043001
[73] Clerici M *et al* 2013 Wavelength scaling of terahertz generation by gas ionization *Phys. Rev. Lett.* **110** 253901
[74] Gaida C, Kienel M, Müller M, Klenke A, Gebhardt M, Stutzki F, Jauregui C, Limpert J and Tünnermann A 2015 Coherent combination of two Tm-doped fiber amplifiers *Opt. Lett.* **40** 2301

Chapter 3

[1] Mourou G A, Tajima T and Bulanov S V 2006 *Rev. Mod. Phys.* **78** 309–71
[2] 2018 Board on Physics and Astronomy, Division on Engineering and Physical Sciences, The National Academies of Sciences, Engineering and Medicine *Opportunities in Intense Ultrafast Lasers: Reaching for the Brightest Light* (The National Academies Press) https://www.nap.edu/catalog/24939/opportunities-in-intense-ultrafast-lasers-reaching-for-the-brightest-light
[3] Falcone R, Albert F, Beg F, Glenzer S, Ditmire T, Spinka T and Zuegel J 2020 arXiv:2002.09712v2
[4] Gales S *et al* 2018 *Rep. Prog. Phys.* **81** 094301
[5] Lureau F *et al* 2020 10 petawatt lasers for extreme light applications *Solid State Lasers XXIX: Technology and Devices* vol 11259 ed W A Clarkson and R K Shori (San Francisco, CA: International Society for Optics and Photonics (SPIE)) pp 283–93
[6] Chang Z 2011 *Fundamentals of Attosecond Optics* (Boca Raton: CRC Press)
[7] McPherson A, Gibson G, Jara H, Johann U, Luk T S, McIntyre I A, Boyer K and Rhodes C K 1987 *J. Opt. Soc. Am.* B **4** 595
[8] Ferray M, L'Huillier A, Li X F, Mainfray G and Manus C 1988 *J. Phys.* B **21** L31
[9] Schafer K J, Yang B, DiMauro L F and Kulander K C 1993 *Phys. Rev. Lett.* **70** 1599
[10] Corkum P B 1993 *Phys. Rev. Lett.* **71** 1994
[11] Rundquist A, III C D, Chang Z, Herne C, Backus S, Murnane M and Kapteyn H C 1998 *Science* **280** 1412
[12] Popmintchev T, Chen M C, Bahabad A, Gerrity M, Sidorenko P, Cohen O, Christov I P, Murnane M M and Kapteyn H C 2009 *Proc. Natl. Acad. Sci.* **106** 10516–21
[13] Han S, Li J, Zhu Z, Chew A, Larsen E W, Wu Y, Pang S S and Chang Z 2020 Advances in atomic, molecular, and optical physics *Chapter One—Tabletop attosecond X-rays in the Water Window* vol 69 ed L F Dimauro, H Perrin and S F Yelin (New York: Academic) pp 1–65

[14] Leone S R *et al* 2014 *Nat. Photon.* **8** 162–6
[15] Shan B and Chang Z 2001 *Phys. Rev.* A **65** 011804
[16] Ren X 2018 *J. Opt.* **20** 023001
[17] Saito N, Sannohe H, Ishii N, Kanai T, Kosugi N, Wu Y, Chew A, Han S, Chang Z and Itatani J 2019 *Optica* **6** 1542–6
[18] Tate J, Auguste T, Muller H G, Salieres P, Agostini P and DiMauro L F 2007 *Phys. Rev. Lett.* **98** 013901
[19] Shiner A D, Trallero-Herrero C, Kajumba N, Bandulet H C, Comtois D, Legare F, Giguere M, Kieffer J C, Corkum P B and Villeneuve D M 2009 *Phys. Rev. Lett.* **103** 073902
[20] Cousin S L, Di Palo N, Buades B, Teichmann S M, Reduzzi M, Devetta M, Kheifets A, Sansone G and Biegert J 2017 *Phys. Rev.* X **7** 041030
[21] Schafer K J, Gaarde M B, Heinrich A, Biegert J and Keller U 2004 *Phys. Rev. Lett.* **92** 23003
[22] Chang Z 2019 *OSA Continuum* **2** 2131–6
[23] Schmidt B E *et al* 2010 *Appl. Phys. Lett.* **96** 121109
[24] Thiré N, Maksimenka R, Kiss B, Ferchaud C, Bizouard P, Cormier E, Osvay K and Forget N 2017 *Opt. Express* **25** 1505–14
[25] Mirov S B, Moskalev I S, Vasilyev S, Smolski V, Fedorov V V, Martyshkin D, Peppers J, Mirov M, Dergachev A and Gapontsev V 2018 *IEEE J. Select. Top. Quant. Electron.* **24** 1–29
[26] Slobodchikov E, Chieffo L R and Wall K F 2016 High peak power ultrafast Cr:ZnSe oscillator and power amplifier *Solid State Lasers XXV: Technology and Devices* vol 9726 ed W A Clarkson and R K Shori (San Francisco, CA: International Society for Optics and Photonics (SPIE)) pp 17–23
[27] Ren X, Mach L H, Yin Y, Wang Y and Chang Z 2018 *Opt. Lett.* **43** 3381–4
[28] Leshchenko V E, Talbert B K, Lai Y H, Li S, Tang Y, Hageman S J, Smith G, Agostini P, DiMauro L F and Blaga C I 2020 *Optica* **7** 981–8
[29] Slobodchikov E and Moulton P F 2011 1-GW-peak-power, Cr:ZnSe laser *CLEO:2011—Laser Applications to Photonic Applications* (Baltimore, MA: Optical Society of America) p PDPA10
[30] Vasilyev S, Peppers J, Moskalev I, Smolski V, Mirov M, Slobodchikov E, Dergachev A, Mirov S and Gapontsev V 2019 1.5-mJ Cr:ZnSe chirped pulse amplifier seeded by a Kerr-lens mode-locked Cr:ZnS oscillator *Laser Congress 2019 (ASSL, LAC, LS&C)* (Optical Society of America) p ATu4A.4
[31] Wu Y, Zhou F, Larsen E W, Zhuang F, Yin Y and Chang Z 2020 *Sci. Rep.* **10** 7775
[32] Migal E, Pushkin A, Bravy B, Gordienko V, Minaev N, Sirotkin A and Potemkin F 2019 *Opt. Lett.* **44** 2550–3
[33] Vallin J, Slack G, Roberts S and Hughes A 1969 *Solid State Commun.* **7** 1211–4
[34] Baranowski J M, Allen J W and Pearson G L 1967 *Phys. Rev.* **160** 627–32
[35] Fazzio A, Caldas M J and Zunger A 1984 *Phys. Rev.* B **30** 3430–55
[36] Colignon D, Kartheuser E, Rodríguez S and Villeret M 1996 *J. Cryst. Growth* **159** 875–8
[37] Mirov S B, Fedorov V V, Martyshkin D, Moskalev I S, Mirov M and Vasilyev S 2015 *IEEE J. Select. Top. Quant. Electron.* **21** 292–310
[38] DeLoach L D, Page R H, Wilke G D, Payne S A and Krupke W F 1996 *IEEE J. Quant. Electron.* **32** 885–95
[39] Page R H, Skidmore J A, Schaffers K I, Beach R J, Payne S A and Krupke W F 1997 Demonstrations of diode—pumped and grating—tuned znse:cr2+ lasers *Advanced Solid State Lasers* (Orlando, FL: Optical Society of America), p LS6

[40] Adams J J, Bibeau C, Page R H, Krol D M, Furu L H and Payne S A 1999 *Opt. Lett.* **24** 1720–2
[41] Xue Y, Xu X, Su L and Xu J 2020 *J. Synth. Cryst.* **49** 1347
[42] Sorokina I T and Sorokin E 2015 *IEEE J. Select. Top. Quant. Electron.* **21** 273–91
[43] Podlipensky A V, Shcherbitsky V G, Kuleshov N V, Levchenko V I, Yakimovich V N, Mond M, Heumann E, Huber G, Kretschmann H and Kück S 2001 *Appl. Phys.* B **72** 253–5
[44] Kanetake T, Hayashi K, Kadoya H, Inayoshi S, Kataoka S, Sugiki F, Nakajima N, Kobayashi R and Kawato S 2018 High efficiency continuous-wave Ti:Sapphire laser *Conference on Lasers and Electro-Optics* (San Jose, CA: Optical Society of America) p JTu2A.92
[45] Zhang W, Teng H, Wang Z, Shen Z and Wei Z 2013 *Appl. Opt.* **52** 1517–22
[46] Kück S 2013 *Recent Development in Laser Crystals with 3D Ions* (Berlin Heidelberg: Springer) pp 1–28
[47] Fedorov V V *et al* 2006 *IEEE J. Quant. Electron.* **42** 907–17
[48] Koechner W 1970 *Appl. Opt.* **9** 2548–53
[49] Lausten R and Balling P 2003 *J. Opt. Soc. Am.* B **20** 1479–85
[50] Chini M, Zhao K and Chang Z 2014 *Nat. Photon.* **8** 178
[51] Mashiko H, Nakamura C M, Li C, Moon E, Wang H, Tackett J and Chang Z 2007 *Appl. Phys. Lett.* **90** 161114
[52] Pushkin A V, Migal E A, Tokita S, Korostelin Y V and Potemkin F V 2020 *Opt. Lett.* **45** 738–41
[53] Yin Y, Ren X, Chew A, Li J, Wang Y, Zhuang F, Wu Y and Chang Z 2017 *Sci. Rep.* **7** 11097
[54] Komm P, Sheintop U, Noach S and Marcus G 2019 *Opt. Express* **27** 18522–32
[55] Baltuška A, Fuji T and Kobayashi T 2002 *Phys. Rev. Lett.* **88** 133901
[56] Yin Y, Li J, Ren X, Zhao K, Wu Y, Cunningham E and Chang Z 2016 *Opt. Lett.* **41** 1142–5
[57] Yin Y, Chew A, Ren X, Li J, Wang Y, Wu Y and Chang Z 2017 *Sci. Rep.* **7** 45794
[58] Strickland D and Mourou G 1985 *Opt. Commun.* **56** 219
[59] Öffner A 1971 *U.S. Patent* 3,748,015 https://www.lens.org/lens/patent/US_3748015_A
[60] Cheriaux G, Rousseau P, Salin F, Chambaret J P, Walker B and Dimauro L F 1996 *Opt. Lett.* **21** 414–6
[61] Treacy E 1969 *IEEE J. Quant. Electron.* **5** 454–8
[62] Martinez O E, Gordon J P and Fork R L 1984 *J. Opt. Soc. Am.* B **1** 1003
[63] Backus S, Durfee C G, Murnane M M and Kapteyn H C 1998 *Rev. Sci. Instrum.* **69** 1207–23
[64] Martinez O 1987 *IEEE J. Quant. Electron.* **23** 1385–7
[65] Tatian B 1984 *Appl. Opt.* **23** 4477–85
[66] Malitson I H 1963 *Appl. Opt.* **2** 1103–7
[67] Vyhlídka Š, Kramer D, Meadows A and Rus B 2018 *Opt. Commun.* **414** 207–11
[68] Maksimenka R *et al* 2010 *Opt. Lett.* **35** 3565–7
[69] Fordell T, Miranda M, Persson A and L'Huillier A 2009 *Opt. Express* **17** 21091–7
[70] Tokita S, Hashida M, Masuno S, Namba S and Sakabe S 2008 *Opt. Express* **16** 14875–81
[71] Nagy T, Simon P and Veisz L 2021 *Adv. Phys.: X* **6** 1845795
[72] Schmidt C, Pertot Y, Balciunas T, Zinchenko K, Matthews M, Wörner H J and Wolf J P 2018 *Opt. Express* **26** 11834–42
[73] Mitrofanov A V *et al* 2015 *Sci. Rep.* **5** 8368
[74] Tochitsky S *et al* 2019 *Nat. Photon.* **13** 41–6
[75] Siegrist F *et al* 2019 *Nature* **571** 240–4

Chapter 4

[1] Nubbemeyer T *et al* 2017 1 kW, 200 mJ picosecond thin-disk laser system *Opt. Lett.* **42** 1381

[2] Schmidt B E, Hage A, Mans T, Légaré F and Worner H J 2017 Highly stable, 54 mJ Yb-InnoSlab laser platform at 0.5 kW average power *Opt. Express* **25** 17549–55

[3] Zapata L E, Reichert F, Hemmer M and Kärtner F X 2016 250 W average power, 100 kHz repetition rate cryogenic Yb:YAG amplifier for OPCPA pumping *Opt. Lett.* **41** 492

[4] Müller M *et al* 2016 1 kW 1 mJ eight-channel ultrafast fiber laser *Opt. Lett.* **41** 3439

[5] Zapata L E *et al* 2015 Cryogenic Yb:YAG composite-thin-disk for high energy and average power amplifiers *Opt. Lett.* **40** 2610

[6] Metzger T *et al* 2009 High-repetition-rate picosecond pump laser based on a Yb:YAG disk amplifier for optical parametric amplification *Opt. Lett.* **34** 2123

[7] Schulz M *et al* 2011 Yb:YAG Innoslab amplifier: efficient high repetition rate subpicosecond pumping system for optical parametric chirped pulse amplification *Opt. Lett.* **36** 2456

[8] Fattahi H *et al* 2016 High-power, 1-ps, all-Yb:YAG thin-disk regenerative amplifier *Opt. Lett.* **41** 1126

[9] Beetar J E, Rivas F, Gholam-Mirzaei S, Liu Y and Chini M 2019 Hollow-core fiber compression of a commercial Yb:KGW laser amplifier *J. Opt. Soc. Am.* B **36** A33

[10] Schenkel B *et al* 2003 Generation of 38-fs pulses from adaptive compression of a cascaded hollow fiber supercontinuum *Opt. Lett.* **28** 1987

[11] Budriūnas R *et al* 2017 53 W average power CEP-stabilized OPCPA system delivering 55 TW few cycle pulses at 1 kHz repetition rate *Opt. Express* **25** 5797

[12] Thiré N *et al* 2018 Highly stable, 15 W, few-cycle, 65 mrad CEP-noise mid-IR OPCPA for statistical physics *Opt. Express* **26** 26907

[13] Thai A, Hemmer M, Bates P K, Chalus O and Biegert J 2011 Sub-250-mrad, passively carrier–envelope-phase-stable mid-infrared OPCPA source at high repetition rate *Opt. Lett.* **36** 3918

[14] Špaček A *et al* 2020 Stability mechanism of picosecond supercontinuum in YAG *Opt. Express* **28** 20205

[15] van de Walle A *et al* 2015 Spectral and spatial full-bandwidth correlation analysis of bulk-generated supercontinuum in the mid-infrared *Opt. Lett.* **40** 673

[16] Indra L *et al* 2017 Picosecond pulse generated supercontinuum as a stable seed for OPCPA *Opt. Lett.* **42** 843

[17] Dubietis A and Couairon A 2019 *Ultrafast Supercontinuum Generation in Transparent Solid-State Media* (Cham: Springer)

[18] Fibich G and Gaeta A L 2000 Critical power for self-focusing in bulk media and in hollow waveguides *Opt. Lett.* **25** 335

[19] Mitschke F M and Mollenauer L F 1986 Discovery of the soliton self-frequency shift *Opt. Lett.* **11** 659

[20] Gordon J P 1986 Theory of the soliton self-frequency shift *Opt. Lett.* **11** 662

[21] Zheltikov A M 2009 Understanding the nonlinear phase and frequency shift of an ultrashort light pulse induced by an inertial third-order optical nonlinearity *Phys. Rev. A: At. Mol. Opt. Phys.* **79** 023823

[22] Gallais L and Commandré M 2014 Laser-induced damage thresholds of bulk and coating optical materials at 1030 nm, 500 fs *Appl. Opt.* **53** A186

[23] Calendron A-L, Çankaya H, Cirmi G and Kärtner F X 2015 White-light generation with sub-ps pulses *Opt. Express* **23** 13866

[24] Weber M J 2018 *Handbook of Optical Materials* (Boca Raton, FL: CRC Press)
[25] Dubietis A, Tamošauskas G, Šuminas R, Jukna V and Couairon A 2017 Femtosekundinio superkontinuumo generavimas plačios apertūros kondensuotose terpėse *Lith. J. Phys.* **57** 113–57
[26] Xu Y and Ching W Y 1999 Electronic structure of yttrium aluminum garnet (formula presented) *Phys. Rev. B: Condens. Matter Mater. Phys.* **59** 10530–5
[27] Kabaciński P, Kardaś T M, Stepanenko Y and Radzewicz C 2019 Nonlinear refractive index measurement by SPM-induced phase regression *Opt. Express* **27** 11018
[28] Boyd R W 2020 The nonlinear optical susceptibility *Nonlinear Optics* (Amsterdam: Elsevier), pp 1–64
[29] Myers L E and Bosenberg W R 1997 Periodically poled lithium niobate and quasi-phase-matched optical parametric oscillators *IEEE J. Quantum Electron.* **33** 1663–72
[30] Powers P E, Kulp T J and Bisson S E 1998 Continuous tuning of a continuous-wave periodically poled lithium niobate optical parametric oscillator by use of a fan-out grating design *Opt. Lett.* **23** 159
[31] Smith D C 1977 High-power laser propagation: thermal blooming *Proc. IEEE* **65** 1679–714
[32] Chen B, Campos J F, Liang W, Wang Y and Xu C Q 2006 Wavelength and temperature dependence of photorefractive effect in quasi-phase-matched $LiNbO_3$ waveguides *Appl. Phys. Lett.* **89** 043510
[33] Buse K, Breer S, Peithmann K, Kapphan S, Gao M and Krätzig E 1997 Origin of thermal fixing in photorefractive lithium niobate crystals *Phys. Rev. B: Condens. Matter Mater. Phys.* **56** 1225–35
[34] Moretti L, Iodice M, Della Corte F G and Rendina I 2005 Temperature dependence of the thermo-optic coefficient of lithium niobate, from 300 to 515 K in the visible and infrared regions *J. Appl. Phys.* **98** 036101
[35] Wu X, Zhou C, Huang W R, Ahr F and Kärtner F X 2015 Temperature dependent refractive index and absorption coefficient of congruent lithium niobate crystals in the terahertz range *Opt. Express* **23** 29729
[36] Hobden M V and Warner J 1966 The temperature dependence of the refractive indices of pure lithium niobate *Phys. Lett.* **22** 243–4
[37] Verluise F, Laude V, Huignard J-P, Tournois P and Migus A 2000 Arbitrary dispersion control of ultrashort optical pulses with acoustic waves *J. Opt. Soc. Am.* B **17** 138–45
[38] Tournois P 1997 Acousto-optic programmable dispersive filter for adaptive compensation of group delay time dispersion in laser systems *Opt. Commun.* **140** 245–9
[39] Zelmon D E, Small D L and Jundt D 1997 Infrared corrected Sellmeier coefficients for congruently grown lithium niobate and 5 mol% magnesium oxide-doped lithium niobate *J. Opt. Soc. Am.* B **14** 3319
[40] Malitson I H 1963 A redetermination of some optical properties of calcium fluoride *Appl. Opt.* **2** 1103
[41] Malitson I H 1965 Interspecimen comparison of the refractive index of fused silica *J. Opt. Soc. Am.* **55** 1205
[42] Michael Bass E V S, DeCusatis C, Enoch J M, Lakshminarayanan V, Li G, MacDonald C and Mahajan V N 2009 *Handbook of Optics, Third Edition Volume IV: Optical Properties of Materials, Nonlinear Optics, Quantum Optics (set)* (New York: McGraw-Hill Professional)
[43] Wang Y *et al* 2020 1.1 J Yb:YAG picosecond laser at 1 kHz repetition rate *Opt. Lett.* **45** 6615–8
[44] Chi H, Wang Y, Davenport A, Menoni C S and Rocca J J 2020 Demonstration of a kilowatt average power, 1 J, green laser *Opt. Lett.* **45** 6803–6

Chapter 5

[1] Laurens H 1928 The physiological effects of radiation *Physiol. Rev.* **8** 1–91

[2] Crowther J 2019 UV reflectance photography of skin–what are you imaging? *Int. J. Cosmet. Sci.* **42** 11

[3] Hearn R M R, Kerr A C, Rahim K F, Ferguson J and Dawe R S 2008 Incidence of skin cancers in 3867 patients treated with narrow-band ultraviolet B phototherapy *Br. J. Dermatol.* **159** 931–5

[4] Wang X, Jiang M, Zhou Z, Gou J and Hui D 2017 3D printing of polymer matrix composites: a review and prospective *Composites* B **110** 442–58

[5] Wu B and Kumar A 2007 Extreme ultraviolet lithography: a review *J. Vac Sci. Technol.* B **25** 1743–61

[6] Savage N 2007 Ultraviolet lasers *Nat. Photon.* **1** 83–5

[7] Franken P A, Hill A E, Peters C W and Weinreich G 1961 Generation of optical harmonics *Phys. Rev. Lett.* **7** 118–9

[8] Hockberger P E 2002 A history of ultraviolet photobiology for humans, animals and microorganisms *Photochem. Photobiol.* **76** 561–79

[9] Engelsen O 2010 The relationship between ultraviolet radiation exposure and vitamin D status *Nutrients* **2** 482–95

[10] Sinha R P and Häder D-P 2002 UV-induced DNA damage and repair: a review *Photochem. Photobiol. Sci.* **1** 225–36

[11] Voet D, Gratzer W B, Cox R A and Doty P 1963 Absorption spectra of nucleotides, polynucleotides, and nucleic acids in the far ultraviolet *Biopolymers* **1** 193–208

[12] Ravanat J-L, Douki T and Cadet J 2001 Direct and indirect effects of UV radiation on DNA and its components *J. Photochem. Photobiol.* B **63** 88–102

[13] Gross A J and Herrmann T R W 2007 History of lasers *World J. Urol.* **25** 217–20

[14] Basting D, Pippert K and Stamm U 2002 History and future prospects of excimer lasers *Second Int. Symp. on Laser Precision Microfabrication* vol 4426

[15] Galli M *et al* 2019 Generation of deep ultraviolet sub-2-fs pulses *Opt. Lett.* **44** 1308–11

[16] McPherson A, Gibson G, Jara H, Johann U, Luk T S, McIntyre I A, Boyer K and Rhodes C K 1987 Studies of multiphoton production of vacuum-ultraviolet radiation in the rare gases *J. Opt. Soc. Am.* B **4** 595–601

[17] Motz H 1951 Applications of the radiation from fast electron beams *J. Appl. Phys.* **22** 527–35

[18] Brabec T and Krausz F 1997 Nonlinear optical pulse propagation in the single-cycle regime *Phys. Rev. Lett.* **78** 3282–5

[19] Seka W, Jacobs S D, Rizzo J E, Boni R and Craxton R S 1980 Demonstration of high efficiency third harmonic conversion of high power Nd-glass laser radiation *Opt. Commun.* **34** 469–73

[20] Beutler M, Ghotbi M, Noack F, Brida D, Manzoni C and Cerullo G 2009 Generation of high-energy sub-20 fs pulses tunable in the 250-310 nm region by frequency doubling of a high-power noncollinear optical parametric amplifier *Opt. Lett.* **34** 710

[21] Baum P, Lochbrunner S and Riedle E 2004 Generation of tunable 7-fs ultraviolet pulses: achromatic phase matching and chirp management *Appl. Phys.* B **79** 1027–32

[22] Baum P, Lochbrunner S and Riedle E 2004 Tunable sub-10-fs ultraviolet pulses generated by achromatic frequency doubling *Opt. Lett.* **29** 1686

[23] Varillas R B, Candeo A, Viola D, Garavelli M, De Silvestri S, Cerullo G and Manzoni C 2014 Microjoule-level, tunable sub-10 fs UV pulses by broadband sum-frequency generation *Opt. Lett.* **39** 3849–52
[24] Tan H-S, Schreiber E and Warren W S 2002 High-resolution indirect pulse shaping by parametric transfer *Opt. Lett.* **27** 439
[25] Polyanskiy M N 2021 Refractive index database https://refractiveindex.info (Accessed 2021-02-02)
[26] Lehmeier H J, Leupacher W and Penzkofer A 1985 Nonresonant third order hyperpolarizability of rare gases and N_2 determined by third harmonic generation *Opt. Commun.* **56** 67–72
[27] Banks P S, Feit M D and Perry M D 1998 High intensity direct third harmonic generation in BBO *Nonlinear Optics'98. Materials, Fundamentals and Applications Topical Meeting (Cat. No. 98CH36244)* (IEEE: Piscataway, NJ), pp 268–70
[28] Gubler U and Bosshard C 2000 Optical third-harmonic generation of fused silica in gas atmosphere: absolute value of the third-order nonlinear optical susceptibility χ (3) *Phys. Rev.* B **61** 10702
[29] Graf U, Fieß M, Schultze M, Kienberger R, Krausz F and Goulielmakis E 2008 Intense few-cycle light pulses in the deep ultraviolet *Opt. Express* **16** 18956–63
[30] Reiter F, Graf U, Serebryannikov E E, Schweinberger W, Fieß M, Schultze M, Azzeer A M, Kienberger R, Krausz F and Zheltikov A M *et al* 2010 Route to attosecond nonlinear spectroscopy *Phys. Rev. Lett.* **105** 243902
[31] Vishnubhatla K C, Bellini N, Ramponi R, Cerullo G and Osellame R 2009 Shape control of microchannels fabricated in fused silica by femtosecond laser irradiation and chemical etching *Opt. Express* **17** 8685–95
[32] Ciriolo A G, Vázquez R M, Roversi A, Frezzotti A, Vozzi C, Osellame R and Stagira S 2020 Femtosecond laser-micromachining of glass micro-chip for high order harmonic generation in gases *Micromachines* **11** 165
[33] Durfee C G III, Rundquist A R, Backus S, Herne C, Murnane M M and Kapteyn H C 1999 Phase matching of high-order harmonics in hollow waveguides *Phys. Rev. Lett.* **83** 2187
[34] Durfee C G, Backus S, Kapteyn H C and Murnane M M 1999 Intense 8-fs pulse generation in the deep ultraviolet *Opt. Lett.* **24** 697
[35] Misoguti L, Backus S, Durfee C G, Bartels R, Murnane M M and Kapteyn H C 2001 Generation of broadband VUV light using third-order cascaded processes *Phys. Rev. Lett.* **87** 013601
[36] Brahms C, Austin D R, Tani F, Johnson A S, Garratt D, Travers J C, Tisch J W G, Russell P S J and Marangos J P 2019 Direct characterization of tuneable few-femtosecond dispersive-wave pulses in the deep UV *Opt. Lett.* **44** 731–4
[37] Travers J C, Grigorova T F, Brahms C and Belli F 2019 High-energy pulse self-compression and ultraviolet generation through soliton dynamics in hollow capillary fibres *Nat. Photon.* **13** 547–54
[38] Brahms C, Belli F and Travers J C 2020 Resonant dispersive wave emission in hollow capillary fibers filled with pressure gradients *Opt. Lett.* **45** 4456
[39] Lekosiotis A, Belli F, Brahms C and Travers J C 2020 Generation of broadband circularly polarized deep-ultraviolet pulses in hollow capillary fibers *Opt. Lett.* **45** 5648
[40] Belli F, Abdolvand A, Chang W, Travers J C and Russell P St 2015 Vacuum-ultraviolet to infrared supercontinuum in hydrogen-filled photonic crystal fiber *Optica* **2** 292

[41] Belli F, Abdolvand A, Travers J C and Russell P St 2019 Highly efficient deep UV generation by four-wave mixing in gas-filled hollow-core photonic crystal fiber *Opt. Lett.* **44** 5509
[42] Trebino R 2000 *Frequency-Resolved Optical Gating: The Measurement of Ultrashort Laser Pulses: The Measurement of Ultrashort Laser Pulses* (Berlin: Springer)
[43] Iaconis C and Walmsley I A 1998 Spectral phase interferometry for direct electric-field reconstruction of ultrashort optical pulses *Opt. Lett.* **23** 792–4
[44] Birge J R, Ell R and Kärtner F X 2006 Two-dimensional spectral shearing interferometry for few-cycle pulse characterization *Opt. Lett.* **31** 2063–5
[45] Li M, Nibarger J P, Guo C and Gibson G N 1999 Dispersion-free transient-grating frequency-resolved optical gating *Appl. Opt.* **38** 5250–3
[46] Witting T, Greening D, Walke D, Matia-Hernando P, Barillot T, Marangos J P and Tisch J W G 2016 Time-domain ptychography of over-octave-spanning laser pulses in the single-cycle regime *Opt. Lett.* **41** 4218–21
[47] Reiter F, Graf U, Schultze M, Schweinberger W, Schröder H, Karpowicz N, Azzeer A M, Kienberger R, Krausz F and Goulielmakis E 2010 Generation of sub-3 fs pulses in the deep ultraviolet *Opt. Lett.* **35** 2248–50
[48] Kida Y 2020 Transient grating in a thin gas target for characterization of extremely short optical pulses *Opt. Lett.* **45** 2231–4
[49] Hazra C, Samanta T and Mahalingam V 2014 A resonance energy transfer approach for the selective detection of aromatic amino acids *J. Mater. Chem.* C **2** 10157–63
[50] Joshi D, Kumar D, Maini A K and Sharma R C 2013 Detection of biological warfare agents using ultra violet-laser induced fluorescence LIDAR *Spectrochim. Acta* A **112** 446–56
[51] Calegari F, Sansone G, Stagira S, Vozzi C and Nisoli M 2016 Advances in attosecond science *J. Phys. B: At. Mol. Opt. Phys.* **49** 062001
[52] Attar A R, Bhattacherjee A, Pemmaraju C D, Schnorr K, Closser K D, Prendergast D and Leone S R 2017 Femtosecond x-ray spectroscopy of an electrocyclic ring-opening reaction *Science* **356** 54–9
[53] Latka T *et al* 2019 Femtosecond wave-packet revivals in ozone *Phys. Rev.* A **99** 063405
[54] Chang K F, Reduzzi M, Wang H, Poullain S M, Kobayashi Y, Barreau L, Prendergast D, Neumark D M and Leone S R 2020 Revealing electronic state-switching at conical intersections in alkyl iodides by ultrafast XUV transient absorption spectroscopy *Nat. Commun.* **11** 4042
[55] Woodward R B and Hoffmann R 1965 Stereochemistry of electrocyclic reactions *J. Am. Chem. Soc.* **87** 395–7
[56] Hoffmann R 1968 Trimethylene and the addition of methylene to ethylene *J. Am. Chem. Soc.* **90** 1475–85
[57] Remacle F and Levine R D 2006 An electronic time scale in chemistry *Proc. Natl Acad. Sci. USA* **103** 6793–8
[58] Calegari F *et al* 2014 Ultrafast electron dynamics in phenylalanine initiated by attosecond pulses *Science* **346** 336–9
[59] Kraus P M *et al* 2015 Measurement and laser control of attosecond charge migration in ionized iodoacetylene *Science* **350** 790–5
[60] Oliver T A A 2018 Recent advances in multidimensional ultrafast spectroscopy *R. Soc. Open Sci.* **5** 171425

[61] Hoi S C, Ganim Z, Jones K C and Tokmakoff A 2007 Transient 2D IR spectroscopy of ubiquitin unfolding dynamics *Proc. Natl Acad. Sci. USA* **104** 14237–42
[62] Consani C, Auböck G, van Mourik F and Chergui M 2013 Ultrafast tryptophan-to-heme electron transfer in myoglobins revealed by UV 2D spectroscopy *Science* **339** 1586–90
[63] Lipman E A, Schuler B, Bakajin O and Eaton W A 2003 Single-molecule measurement of protein folding kinetics *Science* **301** 1233–5
[64] West B A, Womick J M and Moran A M 2011 Probing ultrafast dynamics in adenine with mid-UV four-wave mixing spectroscopies *J. Phys. Chem.* A **115** 8630–7
[65] Tseng C H, Sándor P, Kotur M, Weinacht T C and Matsika S 2012 Two-dimensional Fourier transform spectroscopy of adenine and uracil using shaped ultrafast laser pulses in the deep UV *J. Phys. Chem.* A **116** 2654–61
[66] Chergui M 2019 Ultrafast molecular photophysics in the deep-ultraviolet *J. Chem. Phys.* **150** 070901
[67] Greenfield N J 2007 Using circular dichroism spectra to estimate protein secondary structure *Nat. Protocols* **1** 2876–90
[68] Oppermann M, Bauer B, Rossi T, Zinna F, Helbing J, Lacour J and Chergui M 2019 Ultrafast broadband circular dichroism in the deep ultraviolet *Optica* **6** 56–60
[69] Eppink A T J and Parker D H 1997 Velocity map imaging of ions and electrons using electrostatic lenses: application in photoelectron and photofragment ion imaging of molecular oxygen *Rev. Sci. Instrum.* **68** 3477–84
[70] Nahon L, Garcia G A, Harding C J, Mikajlo E and Powis I 2006 Determination of chiral asymmetries in the valence photoionization of camphor enantiomers by photoelectron imaging using tunable circularly polarized light *J. Chem. Phys.* **125** 114309
[71] Garcia G A, Nahon L, Daly S and Powis I 2013 Vibrationally induced inversion of photoelectron forward-backward asymmetry in chiral molecule photoionization by circularly polarized light *Nat. Commun.* **4** 2132
[72] Turchini S, Catone D, Contini G, Zema N, Irrera S, Stener M, Di Tommaso D, Decleva P and Prosperi T 2009 Conformational effects in photoelectron circular dichroism of alaninol *Chem. Phys. Chem.* **10** 1839–46
[73] Powis I, Harding C J, Garcia G A and Nahon L 2008 A valence photoelectron imaging investigation of chiral asymmetry in the photoionization of fenchone and camphor *Chem. Phys. Chem.* **9** 475–83
[74] Comby A *et al* 2016 Relaxation dynamics in photoexcited chiral molecules studied by time-resolved photoelectron circular dichroism: toward chiral femtochemistry *J. Phys. Chem. Lett.* **7** 4514–9